Article

Fossil isotope evidence for trophic simplification on modern Caribbean reefs

https://doi.org/10.1038/s41586-025-10077-z

Received: 16 April 2025

Accepted: 19 December 2025

Published online: 11 February 2026

Open access

Check for updates

Jessica A. Lueders-Dumont[1,2,3,4,5,8]✉, Aaron O'Dea[1,6,8], Erin M. Dillon[1], Brigida de Gracia[1], Chien-Hsiang Lin[7], Sergey Oleynik[4], Seth Finnegan[1,5], Daniel M. Sigman[4] & Xingchen Tony Wang[2]✉

Caribbean reefs have experienced major human-driven changes to their coral and fish communities[1–4], yet how these changes have affected trophic dynamics remains poorly understood owing to challenges in reconstructing the trophic structure of pre-human-impact reefs. Advances in fossil-bound protein nitrogen isotope ($^{15}N/^{14}N$) analysis now enable the reconstruction of ancient trophic dynamics[5,6], as the ^{15}N to ^{14}N ratio reflects an animal's trophic position[7]. Here we apply this method to modern and prehistoric (7,000-year-old) fish otoliths (ear stones) and corals from Caribbean Panama and the Dominican Republic, focusing on fishes occupying low to middle trophic levels. We find that although the trophic level typically declined in high-trophic-level fishes over time, it increased or remained unchanged in low-trophic-level fishes, indicating that modern food chains are 60–70% shorter than on the prehistoric reefs in both Panama and the Dominican Republic. Furthermore, across all trophic groups, we observed a marked reduction in dietary variation, with a 20–70% lower trophic range on the modern reefs compared to the prehistoric reefs. This pattern is best explained by less dietary specialization in modern reefs, consistent with less ecological complexity than in prehistoric reefs. These differences document and quantify the trophic simplification that has occurred on modern Caribbean reefs, a change that may increase their vulnerability to ecosystem collapse.

Coral reefs are among the most vital marine ecosystems in low-latitude regions. These biodiverse environments provide essential habitats for at least 25% of marine species, including many reef fishes[8]. Moreover, the health of coral reefs is closely linked to the health, storm protection and nutrition of approximately one billion people—about 13% of the global population—who rely on reefs owing to proximity (that is, living within 100 km of coral reefs)[9]. Yet global coral cover across reef ecosystems has declined owing to climate change, eutrophication, overfishing and disease[1,2]. For instance, average stony coral cover in the Caribbean has decreased by 50% since the 1970s[3], leading to a shift from coral- to algae-dominated ecosystems.

One crucial aspect of coral reef biodiversity and resilience is trophic diversity—the range and specialization of feeding roles within the community. Reef fishes perform critical and varied ecological functions, including ectoparasite cleaning, algae farming, symbiotic relationships with invertebrates and poaching[10,11]. Even in fishes considered generalists, high-resolution studies show intraspecific prey specialization[12–14]. This wide range of trophic interactions in these ecosystems underpins their extraordinary biodiversity and productivity[15,16] and thus supports the services that they provide[17].

Despite well-documented losses in coral cover and fish biomass, it remains unclear whether the diets of fish communities have been altered by ecological degradation of coral reefs. Many of the impacts leading to coral reef ecosystem change, including overfishing, eutrophication and shifts in coral community composition, began before modern recordkeeping[3,4]. Thus, reconstructing pre-human trophic structures is critical for understanding whether and how human activities have altered energy flow in these and other marine ecosystems compared to their historical baselines.

Stable isotopes are commonly used in modern ecological studies as tracers of trophic structure and energy flow[7,18]. Recent methodological advancements[5,6,19] have enabled isotopic analyses of organic nitrogen in proteins bound within the fossil skeletons of diverse organisms, including fish otoliths, coral, foraminifera and teeth. These innovations make it feasible to reconstruct past marine food web structure and trophic diversity using an ecosystem-based nitrogen-isotope approach, particularly when multiple taxa co-exist at a given fossil reef site. Otoliths—ear stones involved in vestibular function in bony fishes—have taxon-specific shapes and are composed of calcium carbonate (>99.6% by mass) and organic constituents (<0.4%)[20] (Supplementary Methods). In fossil and subfossil specimens, the mineral lattice protects the organic constituents from factors leading to poor preservation. The high-sensitivity otolith-bound nitrogen isotope ($\delta^{15}N_{oto}$, where $\delta^{15}N = [(^{15}N/^{14}N_{sample})/(^{15}N/^{14}N_{air}) - 1] \times 1{,}000$) approach

[1]Smithsonian Tropical Research Institute, Balboa, Republic of Panama. [2]Department of Earth and Environmental Sciences, Boston College, Chestnut Hill, MA, USA. [3]Tennenbaum Marine Observatories Network, Smithsonian Institution, Edgewater, MD, USA. [4]Department of Geosciences, Princeton University, Princeton, NJ, USA. [5]Department of Integrative Biology, University of California, Berkeley, CA, USA. [6]Sistema Nacional de Investigación (SENACYT), Panama, Republic of Panama. [7]Biodiversity Research Center, Academia Sinica, Taipei, Taiwan. [8]These authors contributed equally: Jessica A. Lueders-Dumont, Aaron O'Dea. ✉e-mail: jessica.lueders-dumont@bc.edu; xingchen.wang@bc.edu

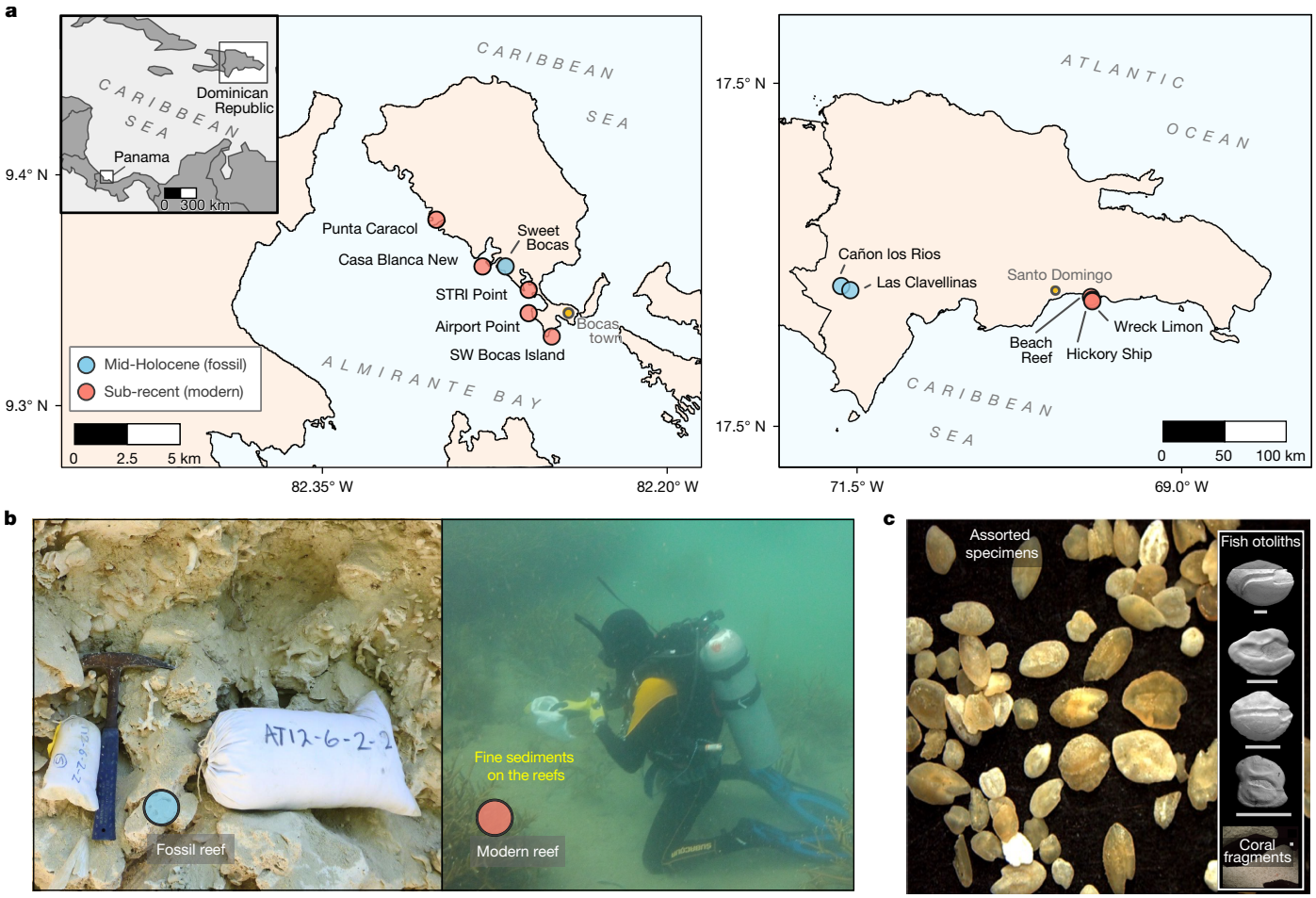

Fig. 1 | Geographic regions and workflow. a, Caribbean regional map and sampling locations within Bocas del Toro, Panama (southwest Caribbean, left) and the Dominican Republic (eastern Caribbean, right) (refer to Extended Data Fig. 1 and Supplementary Table 3 for detailed locality information for modern (red) and fossil (blue) sites). **b**, Sediment sampling of the coral reef framework in modern and fossil coral reefs. **c**, Assorted specimens of coral reef matrix-sourced fossil fish otoliths viewed under a dissecting microscope and inset showing example scanning electron microscopy (SEM) images of the cleaned otoliths and coral skeletal material. From top to bottom in the inset we show representative otoliths from each family (Fig. 2a) in the current study: grunts (Haemulidae), cardinalfishes (Apogonidae), silversides (Atherinidae) and gobies (Gobiidae), with the bottom-most image showing fragments of branching finger coral (Poritidae). Scale bars, 1 mm. Fossil and modern reef images in **b** and images of assorted specimens and otolith SEM in **c** reproduced from ref. 22; PLoS, under a CC0 1.0 Creative Commons license.

enables individual- and community-level $\delta^{15}N$ analyses from fossil specimens but has only begun to be applied to study ecosystems[5,21]. The $\delta^{15}N$ patterns in otoliths—as in muscle tissue—convey information about the proportional contribution of food items with distinct isotopic values (Methods).

Here we measure the $\delta^{15}N$ of fossil-bound organic matter in ~7,000-year-old Caribbean coral reef deposits (Fig. 1), one in Panama (Bocas del Toro) and the other in the Dominican Republic (Enriquillo Basin), to reconstruct coral reef trophic structure before widespread human impacts for comparison with the trophic structure of nearby modern reefs. Fish otoliths and corals are preserved within the coral reef sediments at these sites[22], alongside other biogenic hard parts (for example, spines, denticles, teeth, spicules, shells) from diverse organisms such as molluscs, urchins, sharks and sponges[4]. We focus on coral (*Porites furcata*; family Poritidae) and four fish families (Fig. 2a), gobies (Gobiidae), cardinalfishes (Apogonidae), silversides (Atherinidae) and grunts (Haemulidae), all of which are important prey fish. As prey fish otoliths are primarily deposited onto reef sediments through predator excretion[23], otolith abundances reflect the relative contributions of different fishes to energy flow in the overlying food web averaged over the timescale of sedimentary deposition. These families were therefore chosen for their high abundances in sedimentary deposits as well as their distinct ecological roles. Moreover, apart from grunts, these families are not routinely targeted by fisheries, reducing fishing-driven biases in the dataset[24].

We use $\delta^{15}N$ to quantify three complementary metrics: mean trophic level (MTL; the mean of $\delta^{15}N_{oto}$ measurements for a family or the whole community), isotopic niche width (as reflected by the standard deviation of $\delta^{15}N_{oto}$ measurements for a given family or the whole community[25]) and food chain length (FCL; the range in mean family $\delta^{15}N_{oto}$) (Supplementary Fig. 1). Below, population refers to individual otoliths within a family, whereas community refers to the assemblage of the studied families. Together, these metrics trace fish behaviour, dietary diversity and energy-flow pathways across individuals (each otolith), families (means and variance across individuals within each family) and the partial communities (mean and variance across the families). As diets are averaged within individual fish, high levels of specialization—each fish relying on a distinct subset of prey—can yield relatively large within-family $\delta^{15}N$ variance compared with prey $\delta^{15}N$ variance[14,25]. For example, a large isotopic niche width within a given family, in this context, indicates dietary specialization at the level of individual fish. If fish engage in more generalist foraging, or if resource diversity (that is, the 'menu') has become more homogenous, then we would observe greater trophic similarity among individuals and

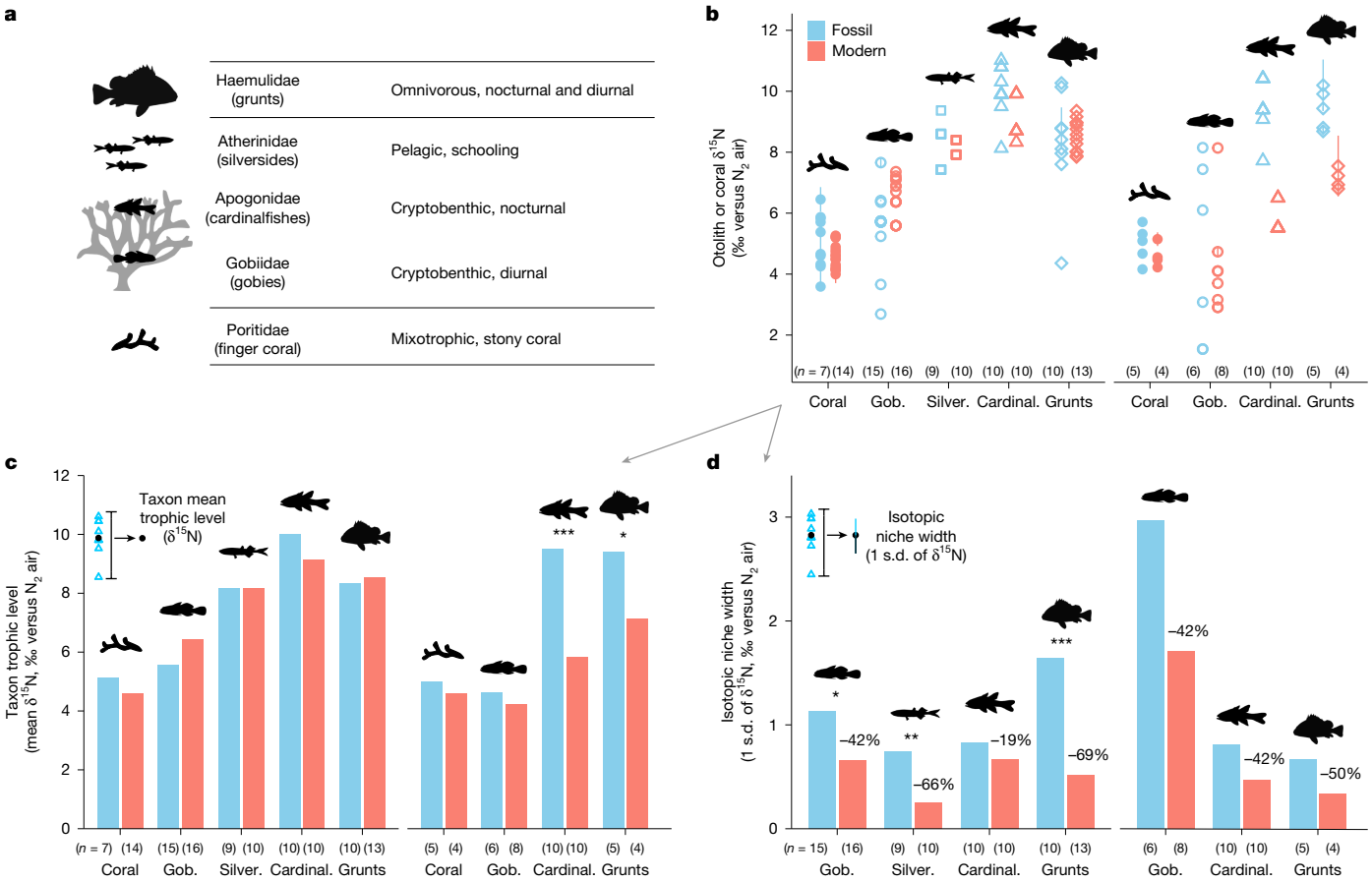

Fig. 2 | Coral- and otolith-bound $\delta^{15}N$ for fossil (~7 ka) and modern (0.1 ka) time periods. a, Descriptions of the taxa analysed in both time periods to generate an ecosystem nitrogen isotope distribution for coral reef trophic reconstruction. Top row: larger reef-associated fishes; middle rows, smaller reef-associated fishes; bottom row, primary consumers. **b**, Measurements of otolith- and coral-bound nitrogen isotopes ($\delta^{15}N$) for each fish family, where each symbol denotes an individual coral fragment or fish otolith. Each symbol represents the mean ± 1 s.d. of replicate measurements from individual otoliths or coral fragments. The *n* value below each category reflects the number of biologically independent individuals (coral fragments or fish) measured for each family, time period and region. **c**, Family-level patterns in $\delta^{15}N$ (trophic level) for fossil and modern time periods (where *n* is the same as for **b**). Statistical tests for whether mean $\delta^{15}N$ has changed since the mid-Holocene are shown below each fish silhouette (Wilcoxon, two-sided; $^{*}P < 0.05$, $^{**}P < 0.01$, $^{***}P < 0.001$). $\delta^{15}N$ declined for Dominican Republic cardinalfishes ($P = 2.5 \times 10^{-4}$, $W = 100$, $r = 0.873$) and grunts ($P = 0.048$, $W = 20$, $r = 0.82$) (Extended Data Table 2). Data from Bocas del Toro, Panama, are shown on the left; data from the southeast Dominican Republic are shown on the right for **b** and **c**. **d**, Regional and family-level patterns in isotopic niche width (diet-driven $\delta^{15}N$ diversity), calculated as the 1 s.d. of the individual-level measurements in **b**. The percent decline compared with the mid-Holocene niche width is shown above each modern bar. Statistical tests for whether the variances have changed since the mid-Holocene are shown below each fish silhouette (*F*-test, two-sided; $^{*}P < 0.05$, $^{**}P < 0.01$, $^{***}P < 0.001$). Panama gobies ($P = 0.043$, $F = 3.0$), silversides ($P = 0.0042$, $F = 8.53$) and grunts ($P = 0.0004$, $F = 10.22$) declined significantly (Extended Data Table 4). Grey arrows (from **b**, pointing towards **c** and **d**) indicate that the metrics shown in **c** (trophic position) and **d** (dietary diversity) are calculated from all data shown in **b**. Insets in each of **c** and **d** illustrate how each metric was calculated. Fish silhouettes in **a**–**d** reproduced from ref. 51, GitHub, under a GPL-2 license.

a narrow within-family isotopic niche width[12,25]. On modern reefs, we predicted that coral loss, predator depletion and habitat fragmentation would reduce resource diversity and promote generalist foraging, leading to greater trophic similarity among individuals. If fish diets also become more similar among families, then FCL is expected to decrease. Ecological theory also predicts that decreased habitat connectivity should lead to decreased FCL[26,27].

We analysed 136 fish otoliths and co-occurring corals from both fossil (mid-Holocene, 7,000 years ago; ka) and modern Caribbean reefs to reconstruct prehistoric and contemporary reef fish trophic structures (Supplementary Table 1). Cleaning and analysis techniques ensured that only fish- and coral-native organic matter was analysed for $\delta^{15}N$ (Methods). The $\delta^{15}N$ of coral-bound organics ($\delta^{15}N_{cb}$) co-varies with regional patterns in the isotopic baseline ($\delta^{15}N_{base}$), that is, the nitrogen isotope composition of nutrients consumed by primary producers at the base of the food chain (Methods). We found that $\delta^{15}N_{base}$ did not change significantly over time in either region (Fig. 2c; Wilcoxon, Panama, $P = 0.45$, $t = 109$, effect size $r = 0.3$; Dominican Republic, $P = 0.62$, $t = 14$, $r = 0.33$; Extended Data Table 1), enabling us to examine trophic-level patterns without adjusting for $\delta^{15}N_{base}$ shifts.

Otolith $\delta^{15}N$ tracks trophic roles

The resulting $\delta^{15}N$ data of fossil fishes (Fig. 2b) generally conformed to expected trophic levels (refer to the '$\delta^{15}N_{oto}$ comparison with known dietary patterns' section in the Supplementary Information), with grunts and cardinalfishes occupying higher trophic levels compared with gobies and silversides. Gobies showed the lowest relative trophic level, consistent with known patterns based on prey items from stomach-content studies[28,29] and tissue-stable-isotope studies (for example, ref. 30) of modern fishes in the Caribbean. Past isotope studies have found that these species were 3–4‰ lower than co-occurring grunts[30], similar to our results. Silversides (small pelagic schooling fishes that primarily consume copepods and fish larvae) had higher $\delta^{15}N$ than gobies, but

lower $\delta^{15}N$ than cardinalfish and grunts. In previous studies, modern silverside tissue $\delta^{15}N$ and trophic level were typically higher than that of co-occurring herbivores[31,32], probably due to the higher $\delta^{15}N$ of pelagic versus benthic organisms in coral reef settings, including in Bocas del Toro, Panama[33]. Thus, the $\delta^{15}N$ elevation of silversides relative to gobies in our study is consistent with pelagic foraging by silversides and primarily benthic foraging by gobies[29]. Grunts, the most abundant representative of higher-trophic-level fishes in our fossil sediment record, are omnivorous or carnivorous predators that move among adjacent habitats, where available, ranging up to 5 km to feed on diverse crustaceans, molluscs and some fish[34,35]. Modern tissue studies on this group of fishes show that their $\delta^{15}N$ ranges from 8–10‰ in the Caribbean, similar to our otolith results[33–35]. Cardinalfishes showed a trophic level that was similar to that of grunts. There are few modern tissue isotope studies on this family[36], but their classification as generalist carnivores is consistent with the relatively high otolith $\delta^{15}N$ observed here. This alignment with known dietary behaviours supports the validity of our fossil trophic-level estimates.

Trophic-level decline in higher-trophic-level fishes

$\delta^{15}N_{oto}$ indicates that the different fish families have experienced different degrees of dietary change since the mid-Holocene (Fig. 2c). In Panama, we observed no significant changes in family trophic levels (Fig. 2c, Extended Data Tables 1 and 2). In the Dominican Republic, modern grunts and cardinalfishes occupied lower trophic levels (that is, had lower average $\delta^{15}N_{oto}$) than their fossil counterparts (Fig. 2c). Specifically, during the modern time period, mean $\delta^{15}N$ was 2.4‰ lower in grunts (Wilcoxon, $P = 0.048$, $W = 20$, $r = 0.82$) and 3.7‰ lower in cardinalfishes ($P = 2.5 \times 10^{-4}$, $W = 100$, $r = 0.873$; Extended Data Table 2). As the trophic level changes in Panama were relatively subtle and required more samples to increase the statistical power, we used a resampling approach to generate bootstrapped $\delta^{15}N$ data (Methods). With the bootstrapped resampling (1,000 iterations), Panama's data echo the changes observed in the Dominican Republic, with higher mid-Holocene $\delta^{15}N$ in grunts and cardinalfishes in Panama, but with a much lower amplitude (grunts: 0.3‰ decline, Wilcoxon, $P = 0.033$, $W = 26$, $r = 0.572$; cardinalfishes: 1.0‰ decline, $P = 2.2 \times 10^{-16}$, $W = 8{,}281$, $r = 0.722$; Extended Data Table 3). Gobies and silversides were similar to or higher than their fossil counterparts in both regions. Specifically, modern goby $\delta^{15}N_{oto}$ was higher than fossil by 1.4‰ (Wilcoxon, $P = 2.2 \times 10^{-16}$, $W = 0$, $r = 0.828$) in Panama and lower by 0.8‰ in the Dominican Republic ($P = 2.2 \times 10^{-16}$, $W = 21{,}732$, $r = 0.840$); silversides were lower by 0.3‰ in Panama ($P = 6.52 \times 10^{-6}$, $W = 1{,}169$, $r = 0.342$) and were not measured in the Dominican Republic owing to a lack of specimens (Extended Data Table 3).

Community shifts in mean trophic level

We also examined community metrics (Fig. 3), including the MTL. Declining MTL in commercial fisheries—termed fishing down the food chain—is well-documented globally, yet most modern studies assume fixed trophic levels for each species, potentially overlooking dynamic changes in trophic level, trophic niche width and FCL. By contrast, nitrogen isotopes capture 'realized' trophic diversity, akin to an Eltonian niche, thus reflecting dynamic patterns in prey availability and consumer behaviour[7,25,37].

Here we estimated MTL in fossil and modern reef fish communities using two approaches: (1) the 'measured MTL' (Fig. 3a) of the partial fish community, calculated by averaging the mean $\delta^{15}N$ values of each of the measured fish families, and (2) the family 'abundance-weighted MTL' (Fig. 3d) that incorporates the numerical abundances of each family (Extended Data Table 5). The latter approach uses the previously described abundances[22] of our target fish groups and applies a resampled (bootstrapped) $\delta^{15}N$ measurement to each individual fish (otolith) recovered from the fossil and modern reefs, generating a modelled family-weighted (or scaled) distribution of fish community $\delta^{15}N$ (refer to the 'Ecosystem nitrogen isotope distribution' section in the Methods). The abundance-weighted MTL is then calculated as the mean of the resulting distribution (Supplementary Fig. 1). As the relative abundances of different component families as well as the measured $\delta^{15}N_{oto}$ can shift the $\delta^{15}N_{oto}$ distribution, the ecosystem nitrogen isotope approach can be considered a dynamic metric for tracking MTL. We included only the three fish families found in both time periods and regions, thus excluding silversides, which were found in high abundances only in Panama.

We found that measured MTL (Fig. 3a) remained stable in Panama (Wilcoxon, $P = 1.0$, $W = 8$, $r = 0$) and in the Dominican Republic (Wilcoxon, $P = 0.4$, $W = 7$, $r = 0.445$) (Fig. 3a, Extended Data Table 2 and Supplementary Table 2). The family abundance-weighted MTL (Fig. 3d), in contrast, increased in Panama from 5.8 to 7.2‰ (Wilcoxon, $P = 2.2 \times 10^{-16}$, $W = 56{,}693$, $r = 0.669$) and decreased in the Dominican Republic from 6.1 to 5.2‰ (Wilcoxon, $P = 8.4 \times 10^{-5}$, $W = 33{,}018$, $r = 0.176$; Extended Data Table 5). Notably, the significant MTL increase in Panama emerged only in the abundance-weighted metric, driven by elevated goby $\delta^{15}N$, which outweighed the $\delta^{15}N$ declines in cardinalfishes and grunts owing to the high abundance of gobies during both time periods (84–91% of the partial community in Panama; Supplementary Tables 4 and 5). The elevated $\delta^{15}N$ of modern gobies is consistent with increased reliance on pelagic prey (refer to the 'Ecological explanations for reduced $\delta^{15}N$ variability' section in the Supplementary Information). In the Dominican Republic, MTL declined owing to the $\delta^{15}N$ declines in each family, although the numerical dominance of gobies (51–95% of the partial community in the Dominican Republic) set the magnitude (0.81‰) of the decline. Goby $\delta^{15}N$ declined only modestly (0.42‰) compared to the larger magnitude declines (2.4‰ in grunts, 3.7‰ in cardinalfishes) in the less abundant taxa, thus yielding the observed 0.81‰ family abundance-weighted MTL decline. We conclude that the comparison of the measured MTL, which is stable through time, to the family-weighted MTL, which showed divergent trends by region, adds context to the ecosystem nitrogen isotope approach for determining changes in reef community trophic structure.

Declines in dietary breadth within taxa

Isotopic niche width (Fig. 2d), calculated from $\delta^{15}N$ variation within each family (1 s.d.; ref. 25) and at the community level (Fig. 3c), was consistently greater in fossil fishes than in modern ones. These niche widths during the mid-Holocene (19 to 69%; Extended Data Table 4) were statistically significant for gobies, silversides and grunts in Panama (*F*-test to compare variances, $P < 0.05$ to $P < 0.001$ depending on species; Extended Data Table 4). No significant niche width changes were observed in the Dominican Republic, probably owing to limited statistical power. Nevertheless, bootstrapped results revealed modern declines in niche widths for Dominican Republic gobies (*F*-test to compare variances, 55% decline, $P < 2.2 \times 10^{-16}$, $F = 4.91$, d.f. = 125) and cardinalfishes (100% decline, $P < 2.2 \times 10^{-16}$, $F = \text{Inf}$, d.f. = 26) and significant shifts in the $\delta^{15}N$ distributions for all Dominican Republic families (Kolmogorov–Smirnov, gobies, $P < 2.2 \times 10^{-16}$, $D = 0.93$; cardinalfishes, $P < 2.2 \times 10^{-16}$, $D = 1$; and grunts, $P = 0.0031$, $D = 1$; Extended Data Table 3).

Within a population, isotopic niche width reflects dietary variation among individual fish. The observed declines therefore suggest a reduction in individual-level dietary specialization on modern reefs (Fig. 3b and Extended Data Table 4). This is consistent with optimal foraging theory[38], which predicts that specialization improves energy efficiency by reducing handling time for each prey item. On degraded modern reefs, limited access to preferred prey probably forces fish to consume a broader array of suboptimal prey, resulting in individuals with more generalized diets[39]. Unintuitively, this leads to narrower population-level isotopic niches, as dietary overlap among individuals increases and $\delta^{15}N$ converges[12,14,25,40] (Fig. 4b). We emphasize that we

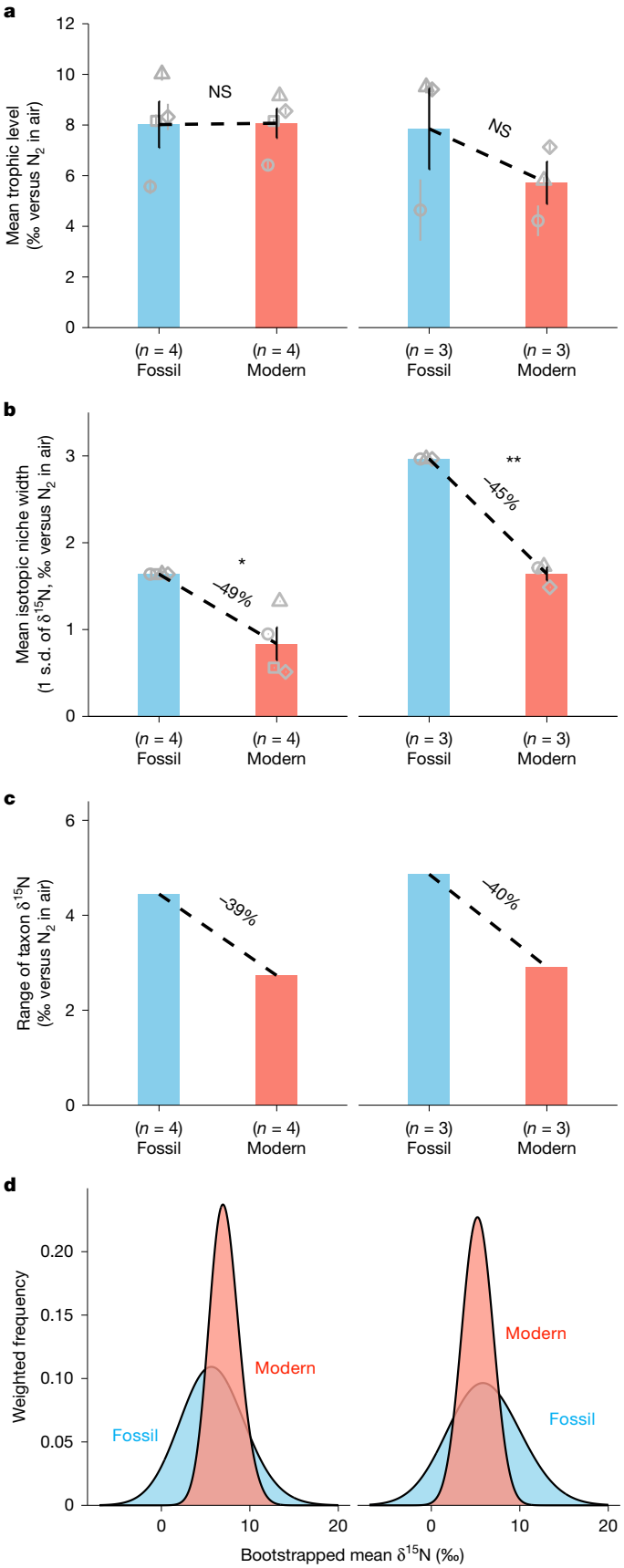

Fig. 3 | Community-level changes. a, Measured MTL, calculated as the mean of mean family $\delta^{15}N$ (±1 s.e.) in each region and time period (where *n* represents families per average) (Supplementary Fig. 1). Measured MTL did not change for Panama (left, Wilcoxon, two-sided, $P = 1$, $W = 8$, $r = 0$) or the Dominican Republic (right, Wilcoxon, $P = 0.4$, $W = 7$, $r = 0.445$) (Extended Data Table 2). Grey symbols show the taxon trophic level (±1 s.e.) (the symbols are the same as for Fig. 2b). NS, not significant. **b**, Isotopic niche width, calculated as the mean of all family s.d. values within each region and time period. To identify changes, we first normalized the isotope niche widths from Fig. 2d. We found that the community mean niche widths declined in both Panama (Paired *t*-test, two-sided, $t = 4.23$, d.f. = 3, $P = 0.0242$) and the Dominican Republic (Paired *t*-test, $t = 17.073$, d.f. = 2, $P = 0.00341$; data were screened for normality using the Shapiro–Wilk test for Panama, $P = 0.42$, $W = 0.90$; and for the Dominican Republic, $P = 0.12$, $W = 0.80$). For modern data, the mean niche ±1 s.e. values are plotted; for the fossil data, no s.e. values are shown because data were scaled to mid-Holocene data from each region, removing variation. Grey symbols show the isotopic niche width for each family (same data as Fig. 2d). **c**, FCL, calculated as the range of mean family $\delta^{15}N$ (see Supplementary Fig. 1). As the FCL is a calculated range, we did not conduct statistical tests. **d**, Family abundance-weighted $\delta^{15}N$ distributions were modelled by applying bootstrapped $\delta^{15}N$ to each otolith in the sedimentary record (refer to the 'Ecosystem nitrogen isotope distribution' section in the Methods). A smoothing function (4× binwidth kernel) was applied to the bootstrapped data to illustrate the distributional changes and therefore focus on the large-scale $\delta^{15}N$ distribution. We calculated community metrics: the family abundance-weighted MTL and the family abundance-weighted FCL (95% interquartile range; Extended Data Table 5 and Supplementary Fig. 1).

observed no niche widening in any family, contrary to predictions from the distributed stress model[41]. This suggests that reduced specialization, not diversification, is the dominant trend.

Alternatively, the narrowing of isotopic niches may reflect a loss in $\delta^{15}N$ diversity among available prey, rather than a behavioural shift in foraging; however, this scenario is less likely, given evidence that many reef fishes increase the number of prey items consumed when preferred prey decline (for example, ref. 39). It is also improbable that remaining prey would coincidentally span a $\delta^{15}N$ range similar to prehistoric means across multiple fish families. In any case, the $\delta^{15}N$ of a prey item generally reflects its trophic position. Thus, regardless of the mechanism, the outcome is the same: increased trophic similarity among individual fish and reduced isotopic niche width at the population level. This emergent pattern highlights a trend towards homogenized trophic roles on modern Caribbean reefs. The decline in family-level niche widths might cause decreased stability as changes in the availability of a given prey item would affect many individual fish in the consumer population[40,42], as discussed below. Overall, the observed changes reveal previously unknown aspects of how human-caused alteration of coral reef ecosystems has affected energy flow on modern reefs, potentially leading to new ecosystem-based indicators of ecosystem health.

Reduced food chain lengths

In both Panama and the Dominican Republic, FCL—the range in mean $\delta^{15}N_{oto}$ across taxa—on the modern reefs was about 40% shorter than during the mid-Holocene (Fig. 3c and Extended Data Table 2). To further assess community-level trophic structure, we calculated FCL from the ecosystem nitrogen isotope distribution (bootstrapped $\delta^{15}N$ data), which uses a resampling approach to weight $\delta^{15}N$ to the proportional abundances of each family (as described above and in the Methods). The analysis (Fig. 3d) revealed a marked decline in community-level $\delta^{15}N$ variance in both regions (Kolmogorov–Smirnov test, $D = 0.91$, $P = 2.2 \times 10^{-16}$ for Panama; $D = 0.47$, $P = 2.2 \times 10^{-16}$ for Dominican Republic; Extended Data Table 5). The modern $\delta^{15}N$ distributions were compressed (Fig. 4), with inter-quartile ranges (95%) reduced by 53% (Panama) and 60% (Dominican Republic) (Extended Data Table 5). The family-weighted distributions show decreased variance (by 2.68–4.05-fold, *F*-test; Panama, $P = 2.2 \times 10^{-16}$, $F = 2.68$, d.f. = 558; Dominican Republic, $P = 2.2 \times 10^{-16}$, $F = 4.04$, d.f. = 158) and had lower kurtosis and skewness (Extended Data Table 5), further recording the contraction of trophic diversity observed in the FCL results.

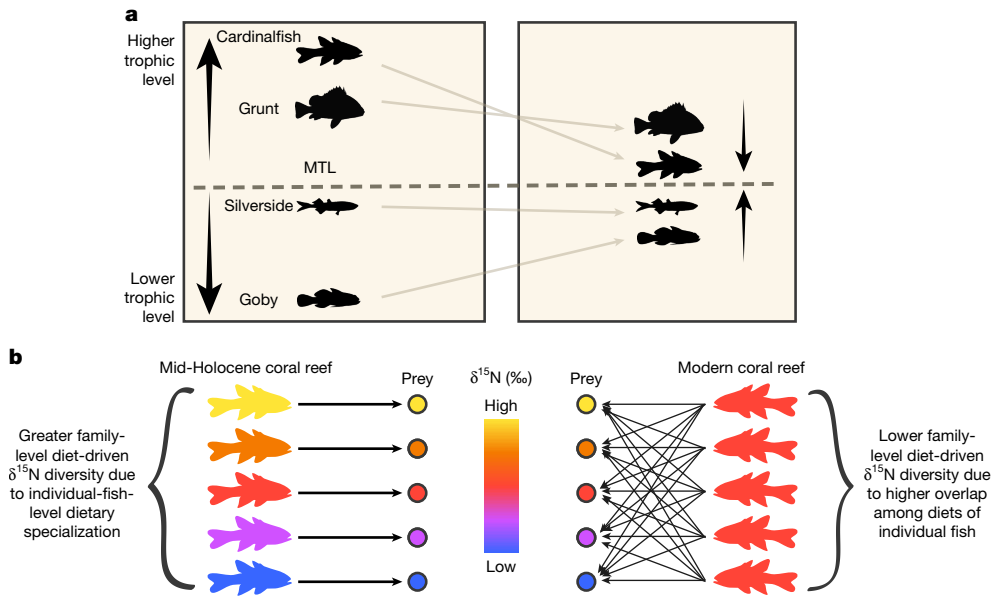

Fig. 4 | Synthesis of reconstructed trophic changes. a, Trophic simplification of modern Caribbean coral reefs. Community patterns in MTL and FCL for the mid-Holocene (left) and modern (right) coral reefs. In the modern reef, FCL declines, whereas community MTL is relatively stable compared with in the fossil reef. **b**, Decreased family-level dietary diversity in modern populations. Individual-fish-level foraging patterns affect family-level isotopic niche width (that is, diet-driven $\delta^{15}N$ diversity). Consuming prey items in common with other fish individuals increases their isotopic similarity to one another, and this isotopic similarity also reflects a homogenization of functional roles and energy flow pathways on coral reefs today. By contrast, fish on mid-Holocene reefs, owing to higher specialization and less overlap, supplied a greater diversity of unique pathways by which energy could enter coral reef food webs. As a greater diversity of energy channels is known to increase food web stability, the loss of heterogeneity on modern reefs may reduce ecosystem stability. Fish silhouettes in **a** and **b** reproduced from ref. 51, GitHub, under a GPL-2 license.

The reduction in FCL reflects a loss of trophic diversity at both the upper and lower extremes of the food web, suggesting a simplification of energy flow pathways among the reef fishes (Fig. 4). This observation might be explained by changes in structural habitat complexity and predation pressure (refer to the 'Ecological explanations for reduced $\delta^{15}N$ variability' section in the Supplementary Information). For example, historically abundant predatory fishes[4] may have created a 'landscape of fear' that constrained prey movement, leading to localized foraging behaviour and supporting fine-scale trophic partitioning[43]. Likewise, greater structural complexity in mid-Holocene coral reefs before human-driven shifts in coral community composition[2,3] probably increased both refugia (from predators) and prey diversity[2,44] by supporting distinct microhabitats with different $\delta^{15}N$ (refs. 36,37). Access to mangrove foraging grounds, which contribute to macroscale habitat complexity and contain relatively high $\delta^{15}N$ prey[34,35], may have further supported longer food chains during the mid-Holocene. In food web theory, declines in habitat connectivity (that is, habitat fragmentation) should generate shorter FCLs[26,27]. As an empirical example of how habitat connectivity affects FCL, coastal habitat fragmentation in the Bahamas results in decreased FCL (and population niche widths) of predators[12]. Fragmentation reduces the diversity of prey, especially higher-trophic-level prey items, decreasing the specialization opportunities for the predators while lowering their trophic level and the ecosystem FCL[12], echoing the results from freshwater ecosystems showing that reduced connectivity decreases the FCL in some contexts[26,27,45]. The greater trophic changes in the Dominican Republic are consistent with the greater intensity of human impacts in the Dominican Republic compared with Panama, including greater losses of mangroves and higher degrees of overfishing[8] (refer to the 'Panama versus Dominican Republic coastal health comparisons' section in the Supplementary Information). Although the relative contribution of each driver (habitat diversity, predator presence, prey availability) is not yet clear, modern coral reef ecosystems clearly show reduced heterogeneity in energy channels.

Importantly, trophic changes were observed across all fish taxa analysed in both regions, including gobies—the lowest trophic level fish species examined. These small, short-lived fishes have outsized roles in energy cycling on coral reefs as both consumers[28,29] and prey[29], comprising up to 80% of fish consumed on coral reefs[46]. Thus, the reconstructed changes in energy flow (prey availability and consumption) would also have impacted the sources, rates and quality of energy supplied to large fishes.

Implications for ecosystem resilience

Using a new 'ecosystem nitrogen isotope' approach that analyses co-existing otolith and coral fossils, this study provides the first direct reconstruction of coral reef fish trophic structure before substantial human impact, and it reveals ecosystem-wide trophic compression across family, community and regional scales. We find that trophic diversity, indicating the breadth of resource use within and across coral reef taxa, has declined markedly. This reduction seems to reflect a loss of dietary specialization and reduced prey availability at the upper and lower ends of food webs.

Our findings show that recent changes on these reefs have shortened reef food chains while also reducing the dietary specialization of reef-associated fishes, similar to comparisons of fished and unfished coral reef food webs in remote oceanic atolls in the Pacific[47]. Modern comparison studies typically find that trophic responses to coral reef degradation are highly context- and species-specific[18,32,48,49] in contrast to our results showing universally reduced niche widths across each family and decreased FCL in both regions.

Our findings have implications for ecosystem stability. The observed family-level shifts in trophic niche width and trophic level suggest that reef fish have already adapted their behaviour to changing prey availability, foraging opportunities and habitat connectivity, demonstrating a degree of resilience (refer to the 'Niche width and ecosystem stability' section in the Supplementary Information). However, as anthropogenic

impacts become progressively more severe, the intrinsic buffering capacity of the food web network is now limited. The reductions in both FCL and niche diversity indicate a contraction in the number of distinct energy pathways that support the ecosystem. Ecological theory predicts that such a decline in diversity can erode stability by weakening the network's ability to buffer shocks[1,27,50]. If all individual fish in a population rely on an overlapping, common pool of resources, as opposed to highly individualized feeding preferences, the population will no longer be buffered against changes in food availability. By contrast, under the mid-Holocene condition of greater intra-population specialization, a given change in food availability would have affected only a subset of individuals. Our reconstruction suggests that modern coral reef ecosystems operate with fewer trophic pathways and reduced functional redundancy, reducing their capacity to withstand ongoing and future stressors and increasing the risk of ecosystem collapse.

Online content

Any methods, additional references, Nature Portfolio reporting summaries, source data, extended data, supplementary information, acknowledgements, peer review information; details of author contributions and competing interests; and statements of data and code availability are available at https://doi.org/10.1038/s41586-025-10077-z.

1. Hughes, T. P. et al. Climate change, human impacts, and the resilience of coral reefs. *Science* **301**, 929–933 (2003).
2. Alvarez-Filip, L., Dulvy, N. K., Gill, J. A., Côté, I. M. & Watkinson, A. R. Flattening of Caribbean coral reefs: region-wide declines in architectural complexity. *Proc. R. Soc. B* **276**, 3019–3025 (2009).
3. Cramer, K. L. et al. Widespread loss of Caribbean Acroporid corals was underway before coral bleaching and disease outbreaks. *Sci. Adv.* **6**, eaax9395 (2020).
4. Dillon, E. M. et al. Fossil dermal denticles reveal the preexploitation baseline of a Caribbean coral reef shark community. *Proc. Natl Acad. Sci. USA* **118**, e2017735118 (2021).
5. Lueders-Dumont, J. A., Wang, X. T., Jensen, O. P., Sigman, D. M. & Ward, B. B. Nitrogen isotopic analysis of carbonate-bound organic matter in modern and fossil fish otoliths. *Geochim. Cosmochim. Acta* **224**, 200–222 (2018).
6. Kast, E. R. et al. Cenozoic megatooth sharks occupied extremely high trophic positions. *Sci. Adv.* **8**, 7–18 (2022).
7. Skinner, C., Cobain, M. R. D., Zhu, Y., Wyatt, A. S. J. & Polunin, N. V. C. Progress and direction in the use of stable isotopes to understand complex coral reef ecosystems: a review. *Oceanogr. Mar. Biol. An Annu. Rev.* **60**, 373–432 (2022).
8. Burke, L., Reytar, K., Spalding, M. & Perry, A. Reefs at risk revisited. *World Resour. Inst.* **74**, 1–130 (2011).
9. Sing Wong, A., Vrontos, S. & Taylor, M. L. An assessment of people living by coral reefs over space and time. *Glob. Chang. Biol.* **28**, 7139–7153 (2022).
10. Aronson, R. B. Foraging behavior of the west Atlantic trumpetfish, *Aulostomus maculatus*: use of large, herbivorous reef fishes as camouflage. *Bull. Mar. Sci.* **33**, 166–171 (1983).
11. Lukoschek, V. & McCormick, M. I. A review of multi-species foraging associations in fishes and their ecological significance. *Proc. Ninth Int. Coral Reef Symp.* **I**, 467–474 (2000).
12. Layman, C. A., Quattrochi, J. P., Peyer, C. M. & Allgeier, J. E. Niche width collapse in a resilient top predator following ecosystem fragmentation. *Ecol. Lett.* **10**, 937–944 (2007).
13. Frédérich, B., Lehanse, O., Vandewalle, P. & Lepoint, G. Trophic niche width, shift, and specialization of *Dascyllus aruanus* in Toliara Lagoon, Madagascar. *Copeia* **2010**, 218–226 (2010).
14. Layman, C. A. & Allgeier, J. E. Characterizing trophic ecology of generalist consumers: A case study of the invasive lionfish in the Bahamas. *Mar. Ecol. Prog. Ser.* **448**, 131–141 (2012).
15. Odum, H. T. & Odum, E. P. Trophic structure and productivity of a windward coral reef community on Eniwetok Atoll. *Ecol. Monogr.* **25**, 291–320 (1995).
16. Polovina, J. J. Model of a coral reef ecosystem: I. The ECOPATH model and its application to French Frigate Shoals. *Coral Reefs* **3**, 1–11 (1984).
17. Woodhead, A. J., Hicks, C. C., Norström, A. V., Williams, G. J. & Graham, N. A. J. Coral reef ecosystem services in the Anthropocene. *Funct. Ecol.* **33**, 1023–1034 (2019).
18. Letourneur, Y., Briand, M. J. & Graham, N. A. J. Coral reef degradation alters the isotopic niche of reef fishes. *Mar. Biol.* **164**, 224 (2017).
19. Wang, X. T. et al. Isotopic composition of carbonate-bound organic nitrogen in deep-sea scleractinian corals: a new window into past biogeochemical change. *Earth Planet. Sci. Lett.* **400**, 243–250 (2014).
20. Lueders-Dumont, J. A. et al. Comparison of the isotopic composition of fish otolith-bound organic N with host tissue. *Can. J. Fish. Aquat. Sci.* **77**, 264–275 (2020).
21. Rao, Z. C. et al. A nitrogen isotopic shift in fish otolith–bound organic matter during the Late Cretaceous. *Proc. Natl Acad. Sci.* **121**, e2322863121 (2024).
22. Lin, C.-H. et al. Reconstructing reef fish communities using fish otoliths in coral reef sediments. *PLoS ONE* **14**, e0218413 (2019).
23. Leonhard, I. & Agiadi, K. Addressing challenges in marine conservation with fish otoliths and their death assemblages. *Geol. Soc. London* **529**, 243–262 (2023).
24. Salas, S., Chuenpagdee, R., Charles, A. T. & Seijo, J. C. *Coastal Fisheries of Latin America and the Caribbean* (Food and Agriculture Organization of the United Nations, 2011).
25. Bearhop, S., Adams, C. E., Waldron, S., Fuller, R. A. & Macleod, H. Determining trophic niche width: a novel approach using stable isotope analysis. *J. Anim. Ecol.* **73**, 1007–1012 (2004).
26. Post, D. M. The long and short of food-chain length. *Trends Ecol. Evol.* **17**, 269–277 (2002).
27. Ward, C. L. & McCann, K. S. A mechanistic theory for aquatic food chain length. *Nat. Commun.* **8**, 2028 (2017).
28. Depczynski, M. & Bellwood, D. R. The role of cryptobenthic reef fishes in coral reef trophodynamics. *Mar. Ecol. Prog. Ser.* **256**, 183–191 (2003).
29. Brandl, S. J., Goatley, C. H. R., Bellwood, D. R. & Tornabene, L. The hidden half: ecology and evolution of cryptobenthic fishes on coral reefs. *Biol. Rev.* **93**, 1846–1873 (2018).
30. Zhu, Y., Newman, S. P., Reid, W. D. K. & Polunin, N. V. C. Fish stable isotope community structure of a Bahamian coral reef. *Mar. Biol.* **166**, 160 (2019).
31. Tilley, A., López-Angarita, J. & Turner, J. R. Diet reconstruction and resource partitioning of a Caribbean marine mesopredator using stable isotope Bayesian modelling. *PLoS ONE* **8**, e79560 (2013).
32. Hempson, T. N. et al. Coral reef mesopredators switch prey, shortening food chains, in response to habitat degradation. *Ecol. Evol.* **7**, 2626–2635 (2017).
33. Stuthmann, L. E. & Castellanos-Galindo, G. A. Trophic position and isotopic niche of mangrove fish assemblages at both sides of the Isthmus of Panama. *Bull. Mar. Sci.* **96**, 449–467 (2020).
34. Vaslet, A., Phillips, D. L., France, C. A. M., Feller, I. C. & Baldwin, C. C. Trophic behaviour of juvenile reef fishes inhabiting interlinked mangrove-seagrass habitats in offshore mangrove islets. *J. Fish Biol.* **87**, 256–273 (2015).
35. Cocheret de la Morinière, E. et al. Ontogenetic dietary changes of coral reef fishes in the mangrove-seagrass-reef continuum: stable isotopes and gut-content analysis. *Mar. Ecol. Prog. Ser.* **246**, 279–289 (2003).
36. Frédérich, B. et al. Comparative feeding ecology of cardinalfishes (Apogonidae) at Toliara reef, Madagascar. *Zool. Stud.* **56**, e10 (2017).
37. Rader, J. A. et al. Isotopic niches support the resource breadth hypothesis. *J. Anim. Ecol.* **86**, 405–413 (2017).
38. Schoener, T. W. Theory of feeding strategies. *Annu. Rev. Ecol. Syst.* **2**, 369–404 (1971).
39. Clever, F. et al. The gut microbiome variability of a butterflyfish increases on severely degraded Caribbean reefs. *Commun. Biol.* **5**, 770 (2022).
40. Stewart, S. D., Kelly, D., Biessy, L., Laroche, O. & Wood, S. A. Individual diet specialization drives population trophic niche responses to environmental change in a predator fish population. *Food Webs* **27**, e00193 (2021).
41. Steube, T. R., Altenritter, M. E. & Walther, B. D. Distributive stress: individually variable responses to hypoxia expand trophic niches in fish. *Ecology* **102**, e03356 (2021).
42. Stouffer, D. B. & Bascompte, J. Compartmentalization increases food-web persistence. *Proc. Natl Acad. Sci. USA* **108**, 3648–3652 (2011).
43. Hixon, M. A. & Beets, J. P. Predation, prey refuges, and the structure of coral-reef fish assemblages. *Ecol. Monogr.* **63**, 77–101 (1993).
44. Beukers, J. S. & Jones, G. P. Habitat complexity modifies the impact of piscivores on a coral reef fish population. *Oecologia* **114**, 50–59 (1998).
45. Tunney, T. D., McCann, K. S., Lester, N. P. & Shuter, B. J. Food web expansion and contraction in response to changing environmental conditions. *Nat. Commun.* **3**, 1105 (2012).
46. Brandl, S. J. et al. Demographic dynamics of the smallest marine vertebrates fuel coral reef ecosystem functioning. *Science* **364**, 1189–1192 (2019).
47. Young, H. S., McCauley, F. O., Micheli, F., Dunbar, R. B. & McCauley, D. J. Shortened food chain length in a fished versus unfished coral reef. *Ecol. Appl.* **34**, e3002 (2024).
48. Morillo-Velarde, P. S. et al. Habitat degradation alters trophic pathways but not food chain length on shallow Caribbean coral reefs. *Sci. Rep.* **8**, 4109 (2018).
49. Briones-Fourzán, P. et al. Coral reef degradation differentially alters feeding ecology of co-occurring congeneric spiny lobsters. *Front. Mar. Sci.* **5**, 516 (2019).
50. Schindler, D. E. et al. Population diversity and the portfolio effect in an exploited species. *Nature* **465**, 609–612 (2010).
51. Schiettekatte, N. M. D., Brandl, S. J. & Casey, J. M. *fishualize: Color Palettes Based on Fish Species* (GitHub, 2019); https://nschiett.github.io/fishualize/index.html.

Methods

Taxa

Our main goal was to assess long-term changes in the trophic structure of coral reef-associated fishes compared to prehistoric trophic structure before widespread human impacts. As different stressors can affect different components of marine food webs, we analysed otoliths from key taxa representing the most abundant species from different ecological niches. Gobies (Gobiidae) are abundant, small, cryptobenthic fishes that forage in reef crevices. Cardinalfishes (Apogonidae) are cryptobenthic taxa that exhibit nocturnal off-reef foraging[29]. Silversides (Atherinidae) are small, pelagic planktivores that feed in schools above reefs[52] and grunts (Haemulidae) are relatively larger omnivores that forage in both reef and adjacent seagrass and mangrove habitats[35]. For taxonomic identification based on otoliths, we used a Caribbean otolith reference collection comprised of locally obtained modern specimens[22]. Owing to the diagnostic limitations of identifying very small otoliths from early life history stages, only a portion (30–100%, depending on the family; Supplementary Table 4) could be identified to the genus or species, whereas the remaining specimens were assigned to family (8–60%).

Study regions

Otoliths were extracted from two coral reef sedimentary deposits that are the only known mid-Holocene otolith-bearing reef sediments in the Caribbean, located in Bocas del Toro, Panama (9° N × 82° W; Fig. 1 and Supplementary Table 3), and the Enriquillo Basin, Dominican Republic (18° N × 71° W). These sites contain well-preserved fossil reef assemblages spanning the mid-Holocene (around 7000 years before present; BP) and modern (around 100 BP) time periods[22,53]. Multiple sub-localities were sampled in each region (Extended Data Fig. 1). Bulk sediments, around 9 kg per sample, were collected from reef frameworks using different methods depending on the time period as described in ref. 22. At the mid-Holocene sites, sediments were excavated from 3-m-deep trenches, whereas in modern reefs, SCUBA divers collected sediment from 10–15-cm-deep strata adjacent to living corals. Samples were sieved into size fractions (2 mm, 500 μm, 250 μm and 106 μm) and then otoliths were manually extracted under a dissecting microscope.

Dating

Radiometric dating of coral skeletal material using U-Th and calibrated radiocarbon techniques was previously published for Panama[4,22,53] and the Dominican Republic[54–56]. For both regions and time periods, fossil samples spanned around 100 years. U-Th dates showed a larger date range than ages obtained from radiocarbon dating, with ages falling between 6345 and 7164 BP (819 y range) for U-Th, and between 6533 to 6638 BP for ^{14}C (105 y range[4]). Similarly, dates for the modern samples ranged from 1152 to 1984 BP (832 year range[3]) for U-Th, with the majority of ^{14}C dates between 1926 to 2014 CE for modern (that is, approximately the past 100 years[22,53,57]).

Otolith specimen selection

We selected otolith and coral specimens across multiple reef sub-localities to capture spatial and temporal variability (Supplementary Table 3). In total, 91 fish otolith specimens were analysed from Panama (42 mid-Holocene, 49 modern) and 42 from the Dominican Republic (21 mid-Holocene, 21 modern). To select otoliths from the collection, a list of sample numbers (specifying a unique combination of locality + depth + bulk bag replicate) were selected on the basis of obtaining samples from a wide distribution of sub-localities in each region. Otoliths were then randomly chosen from each sample number until $n = 10–30$ otoliths for each taxon from each country and time period were selected (Supplementary Fig. 2 shows the spatial distribution of specimens across different sub-localities). Localities close to banana plantations (for example, Punto Donato) were avoided, as were sites with known time-averaging problems (Airport Point) or distinct exposures (Cayo Adriana, which is oceanographically connected); however, for Atherinidae and Haemulidae, samples were needed from each of these localities for sufficient sample size.

Furthermore, five modern grunts (family Haemulidae) were measured from the reference collection. Other reef fishes ($n = 35$) were also measured but not included owing to a lack of conspecifics for comparison, including fishes in the Engraulidae (21), Lutjanidae (8), Serranidae (4) and Gerreidae (2) families (Supplementary Fig. 3). These data were not included in the main text owing to a lack of comparisons across time periods or regions.

Coral specimen selection

The ecosystem nitrogen isotope approach allowed for direct comparisons of fish-trophic-level shifts using otolith-bound δ^{15}N from multiple taxa while controlling for possible isotopic baseline δ^{15}N variability using coral-bound δ^{15}N. $\delta^{15}N_{cb}$ patterns are known to reflect variations in $\delta^{15}N_{base}$, the nitrogen isotope composition of nutrients consumed by primary producers at the base of the food chain[58,59]. Although corals are mixotrophic, and heterotrophic feeding can increase the δ^{15}N due to decreased reliance on symbionts[60], the primary signal is the δ^{15}N of inorganic nutrients[58,61,62]. We used coral fragments (as per ref. 63), allowing for similar spatiotemporal sampling of otoliths and corals across sites. We analysed fragments ($n = 3–5$ per locality and time period) of branching *Porites furcata* (Panama, $n = 26$; Dominican Republic, $n = 9$). Where possible, coeval corals and otoliths from the same sub-localities and depth horizons bags were analysed (Supplementary Fig. 2 and Fig. 3).

Pre-processing of coral and otolith specimens

Three regions of each coral fragment were exposed with a rotary disk drill (Dremel 4000) and visually inspected for encrusting organisms. Powders were removed by drilling with a rotary tool using a 1.4 mm diamond drill bit (Shofu). The powder drilled from each fragment was homogenized and subsampled into two subsamples that were analysed separately for coral-bound δ^{15}N using previously established methods[19,58]. Subsamples were then averaged to generate a mean value for each coral fragment.

Otoliths were photographed (Leica KL1500 LCD), weighed and prepared for δ^{15}N analysis. Specimens were pulverized and homogenized before chemical cleaning, following established protocols[5]. Otoliths with initial masses of over 5.5 mg were subsampled into masses between 3.5 and 4.5 mg. For otoliths with initial masses of less than 5.5 mg, the otolith was pulverized and the powder from the entire otolith was analysed. Initial nitrogen isotope analyses involved pooled otoliths (Extended Data Fig. 2) to ensure sufficient nitrogen content for measurements out of an abundance of caution to ensure sufficient nitrogen for analysis. All subsequent isotopic analyses were conducted on individual otoliths, including specimens as small as 0.06 mg (60 μg) (Supplementary Table 1).

Previous studies show that the δ^{15}N patterns in otoliths—for example, muscle tissue—convey information about the proportional contribution of food items with distinct isotopic values[64]. This method has been validated through calibration studies showing consistent trophic information compared with the commonly measured tissues[20,64]. $\delta^{15}N_{oto}$ studies have reconstructed trophic information on centennial and million-year timescales[5].

δ^{15}N measurements

For coral and otolith powders, cleaning of the biomineral powder entailed sequential treatments with sodium polyphosphate (clay removal), dithionite-citric acid (metal oxide removal) and sodium hypochlorite (non-bound organic removal), as described in ref. 19 and ref. 5. Once cleaned, powdered samples were dissolved in ACS-grade 4 N HCl, and organic nitrogen was oxidized with basic persulfate oxidizing

reagent. Nitrate concentrations were determined using chemiluminescence[65]. To convert nitrate to N_2O, sample aliquots amounting to 10 nmol nitrogen were injected into vials of concentrated denitrifying bacteria and digested at room temperature for 3–6 h (refs. 66,67). The ^{15}N to ^{14}N ratio of the sample analyte, N_2O, was analysed on a MAT253 GC-IRMS interfaced with a purpose-built N_2O purification and extraction system at Princeton University (Isodat v.3.0)[66,67]. Long-term analytical precision (1 s.d.) was 0.08‰ for N_2O standards and 0.3‰ for in-house otolith standards.

Food web metrics

To assess shifts in trophic structure, we calculated several metrics (Supplementary Fig. 1). For each family, we calculated the taxon trophic level and the isotopic niche width (1 s.d.; for example, ref. 68). For the fish community, we report (1) the MTL, which is calculated as the mean of each family's trophic level, and (2) the FCL, the number of trophic steps in the food web, calculated as the isotopic difference between the lowest- and highest-trophic-level family means from each time period and region. Our calculations, based on family-level trophic-level as opposed to the trophic-level of individual fish, are a conservative measure of the trophic distance between the highest- and lowest-trophic-level taxa due to the low sample sizes of the fish measured. Isotopic niche width, calculated as the variation (1 s.d.) in $\delta^{15}N$ within each family, is an indicator of breadth—that is, the dietary dissimilarity—of the community. Baseline-corrected $\delta^{15}N$ were standardized by the respective regional (Panama or Dominican Republic) and temporal $\delta^{15}N_{cb}$ (Extended Data Table 2). As FCL is a relative, not absolute metric, baseline $\delta^{15}N$ does not affect its value.

When examining our data by species- and genus-level, where otolith-based identification allowed for higher taxonomic resolution, we found that $\delta^{15}N$ followed the same patterns as the family-level $\delta^{15}N$ patterns (Extended Data Fig. 3). DNA metabarcoding of stomach contents also supports this observation, showing that family-level patterns in coral reef fish diet are consistently better predictors of fish diet than trophic group or guild[69,70]. Consequently, for the purposes of interpreting the family-level isotope data, family-level patterns can be considered indicators of species- or population-level trophic patterns.

Potential artifacts—such as changes in fish community composition, differences in sample time averaging or preservation-related effects on $\delta^{15}N$—could influence family- or community-level patterns (refer to the 'Community composition', 'Time averaging' and 'Preservation' sections in the Supplementary Information). Shifts in the size distribution of the sampled fishes could also influence trophic structure, as size and trophic level are tightly linked in most fish (refer to the 'Fish size' section in the Supplementary Information); however, our collected samples reveal consistency in each variable, suggesting stable species distributions, temporal sampling (80–100 years; refer to the 'Dating' section above), fish size (Extended Data Fig. 4a and Supplementary Fig. 4) and preservation (Extended Data Fig. 4b and Supplementary Fig. 5) across periods. Thus, consistent with previous studies showing fossil versus modern declines in aspects of coral reef ecosystem health in the region (Supplementary Fig. 6), the trophic changes are more likely explained by the multiple stressors acting upon modern coral reefs.

Ecosystem nitrogen isotope distribution

To assess the impacts of our observed $\delta^{15}N$ changes at the scale of the fish community, we modelled taxon-weighted distributions of $\delta^{15}N$ for each region and time period. Community composition data was used to weight the $\delta^{15}N$ to generate a model of community-weighted $\delta^{15}N$ distributions. Matrices containing the proportional contributions of each of the three taxonomic groups found in both regions for both time periods—gobies, grunts and cardinalfishes—and their corresponding mean and median $\delta^{15}N$ were used to model $\delta^{15}N$ distribution at the community level (Supplementary Table 5).

Pseudo-replicated $\delta^{15}N$ values (that is, for samples where multiple otoliths were combined to make one measurement and each otolith treated separately for the purposes of the main text) were removed before calculating the means and medians. To minimize the influence of outliers, localities with $n \leq 2$ were excluded. The mean $\delta^{15}N$ was calculated from the raw data in those cases.

To obtain proportional contributions, each locality was treated as a sample owing to the low otolith counts in some sub-locality bulk sample bags. Then, the proportions were averaged across all localities within each period and region.

Bootstrapped sampling distributions were generated to capture more of the variation across $\delta^{15}N$ measurements. For each family-region-age group, the original $\delta^{15}N$ values were sampled (sample size $n = 100$) with replacement, and a mean was calculated from each bootstrapped sample (with $n = 1{,}000$ iterations). This generated a distribution of means for each group, from which values were randomly pulled and then assigned to each otolith found in the bulk samples. The new distributions were then plotted from these values. Following these analyses, we provide a figure summarizing the patterns observed in each region (Supplementary Fig. 7).

Statistics

We used R (R Core Team, 2024) to perform statistical tests and plot our data. Fish shapes for grunts, gobies and cardinalfishes were obtained from the R package fishualize[51] (v.0.2.3). All data analysis was conducted using R software (v.4.1.2), via the tidyverse (v.1.3.1), boot (v.1.3-28), rlist (v.0.4.6.2), onewaytests (v.2.7), rstatix (v.0.7.0), forcats (v.0.5.1) and tidyr (v.1.3.1) packages. We used the following packages for other statistical and mapping operations in R: ggmap (v.3.0.0), ggrepel (v.0.9.3), ggsn (v.0.5.3), cowplot (v.1.1) and grid (v.4.1.1).

Reporting summary

Further information on research design is available in the Nature Portfolio Reporting Summary linked to this article.

Data availability

All data used in this study are available from FigShare at https://doi.org/10.6084/m9.figshare.28811663.

Code availability

The code used for bootstrapping (Fig. 3d and Extended Data Fig. 5) and other R scripts used to create figures are available at https://doi.org/10.6084/m9.figshare.28811663.

52. Randall, J. *Food Habits of Fishes of the West Indies* (NOAA, 1967).
53. O'Dea, A. et al. Defining variation in pre-human ecosystems can guide conservation: an example from a Caribbean coral reef. *Sci. Rep.* **10**, 2922 (2020).
54. Mann, P., Taylor, F. W., Burke, K. & Kulstad, R. Subaerially exposed Holocene coral reef, Enriquillo Valley, Dominican Republic. *Bull. Geol. Soc. Am.* **95**, 1084–1092 (1984).
55. Greer, L. & Swart, P. K. Decadal cyclicity of regional mid-Holocene precipitation: evidence from Dominican coral proxies. *Paleoceanography* **21**, PA2020 (2006).
56. Cuevas, D. N., Sherman, C. E., Ramírez, W. & Hubbard, D. K. Coral growth rates from the Holocene Cañada Honda fossil reef, southwestern Dominican Republic: comparisons with modern counterparts in high sedimentation settings. *Caribb. J. Sci.* **45**, 94–109 (2009).
57. Fredston-Hermann, A. L., O'Dea, A., Rodriguez, F., Thompson, W. G. & Todd, J. A. Marked ecological shifts in seagrass and reef molluscan communities since the mid-Holocene in the southwestern Caribbean. *Bull. Mar. Sci.* **89**, 983–1002 (2013).
58. Wang, X. T. et al. Isotopic composition of skeleton-bound organic nitrogen in reef-building symbiotic corals: a new method and proxy evaluation at Bermuda. *Geochim. Cosmochim. Acta* **148**, 179–190 (2015).
59. Wang, X. T. et al. Influence of open ocean nitrogen supply on the skeletal $\delta^{15}N$ of modern shallow-water scleractinian corals. *Earth Planet. Sci. Lett.* **441**, 125–132 (2016).
60. Donnelly, H. A. et al. Groundtruthing nitrogen isotopes as a symbiosis proxy using the facultatively symbiotic coral *Oculina arbuscula*. *Front. Mar. Sci.* **11**, 1433382 (2024).
61. Luu, V. H. et al. Nitrogen isotope ratios across the Bermuda coral reef: implications for coral nitrogen sources and the coral-bound nitrogen isotope proxy. *Front. Mar. Sci.* **12**, 1554418 (2025).
62. Sims, Z. C., Cohen, A. L., Luu, V. H., Wang, X. T. & Sigman, D. M. Uptake of groundwater nitrogen by a near-shore coral reef community on Bermuda. *Coral Reefs* **39**, 215–228 (2020).

63. Wang, X. T. et al. Deep-sea coral evidence for lower Southern Ocean surface nitrate concentrations during the last ice age. *Proc. Natl Acad. Sci. USA* **114**, 3352–3357 (2017).
64. Lueders-Dumont, J. A. et al. Controls on the nitrogen isotopic composition of fish otolith organic matter: lessons from a controlled diet switch experiment. *Geochim. Cosmochim. Acta* **316**, 69–86 (2022).
65. Braman, R. S. & Hendrix, S. A. Nanogram nitrite and nitrate determination in environmental and biological materials by vanadium (III) reduction with chemiluminescence detection. *Anal. Chem.* **61**, 2715–2718 (1989).
66. Sigman, D. M. et al. A bacterial method for the nitrogen isotopic analysis of nitrate in seawater and freshwater. *Anal. Chem.* **73**, 4145–4153 (2001).
67. Weigand, M. A., Foriel, J., Barnett, B., Oleynik, S. & Sigman, D. M. Updates to instrumentation and protocols for isotopic analysis of nitrate by the denitrifier method. *Rapid Commun. Mass Spectrom.* **30**, 1365–1383 (2016).
68. Boecklen, W. J., Yarnes, C. T., Cook, B. A. & James, A. C. On the use of stable isotopes in trophic ecology. *Annu. Rev. Ecol. Evol. Syst.* **42**, 411–440 (2011).
69. Casey, J. M. et al. Reconstructing hyperdiverse food webs: gut content metabarcoding as a tool to disentangle trophic interactions on coral reefs. *Methods Ecol. Evol.* **10**, 1157–1170 (2019).
70. Parravicini, V. et al. Delineating reef fish trophic guilds with global gut content data synthesis and phylogeny. *PLoS Biol.* **18**, e3000702 (2020).
71. Kahle, D. & Wickham, H. ggmap: spatial visualization with ggplot2. *R J.* **5**, 144–161 (2013).

Acknowledgements This work was funded by the Smithsonian MarineGEO programme (J.A.L.-D.); the Smithsonian Tropical Research Institute (J.A.L.-D. and A.O.); the Smithsonian Institution Scholarly Studies (A.O.); the US National Science Foundation through grants EAR-2347773 (A.O., B.D.G., E.M.D. and S.F.) and EAR-1325683 (A.O.); the Secretaría Nacional de Ciencia Tecnología e Innovación, Panamá (A.O., E.M.D., B.D.G. and J.A.L.-D.); the Scott Fund of the Department of Geosciences, Princeton University (J.A.L.-D.); the David and Lucile Packard Foundation (S.F.); the Army Engineer Research and Development Center through grants W912HZ2020061-RA2 and W912HZ2520020 (J.A.L.-D., X.T.W.); the Simons Foundation through Grant No. 00016323 (X.T.W.); and Boston College start-up funds (X.T.W.). We are grateful to the Anders, Bytnar and Selin families for donations that supported Panama field and laboratory work. We acknowledge the logistical and technical support from the following people: A. Bilgray, P. Gomez, M.R. Russo, E. Groves, N. Zelizer, S. Castillo, F. Rodriguez, M. Lepore, O. Aguilera, S. Mattson, M. Hynes, S. dos Santos, M. Alvarez, P. Gondola, U. Gonzalez, J. Edlinger, D. Doughty, E. Grossman, G. Jacome, G. Abreu, V. Galvan, R. de Leon, Y. del Valle, G. Quijano, K. Griswold, K. Ripley-Dunlap, I. Ingemi, C. Vergara-Chan, A. Verdurmen, M. Pinzon, M. Herrera, R. Robertson, D. Cedeño, K. McComas, Y. Samara, C. Courtier, M. Ureña, H. Hernández, C. De Leon, J. Mate, R. Torres and the team at Sweet Bocas, Panama. We thank S.F. Gale for discussion and insights regarding Fig. 4. Collection permits for bulk sediment sampling were issued by the Ministerio de Ambiente, República de Panamá (permit SE/AO-4-18) and the Ministerio de Medio Ambiente y Recursos Naturales, República Dominicana (permit VAPB-02374). Goby, cardinalfish and grunt silhouettes are from the R package fishualize (v.0.2.3); branching coral outlines in Fig. 1b are from D. Kleine, Marine Botany UQ (ian.umces.edu/media-library) under the Attribution-ShareAlike 4.0 International (CC BY-SA 4.0) license (https://creativecommons.org/licenses/by-sa/4.0/#). This is contribution 158 from the Smithsonian's MarineGEO and Tennenbaum Marine Observatories Network.

Author contributions This study was designed by J.A.L.-D. and A.O. with input from B.D.G., X.T.W., E.M.D. and D.M.S. Field and sediment sampling was done by B.D.G. and A.O. Taxonomic identification was done by B.D.G. and C.-H.L. J.A.L.-D. sampled the material and conducted the isotope analysis with help from S.O. J.A.L.-D. and E.M.D. performed the statistical analysis with input from A.O., X.T.W., S.F. and D.M.S. J.A.L.-D., A.O. and X.T.W wrote the manuscript with input from all authors. All authors were involved in discussion of the data at different stages and contributed to the final manuscript.

Competing interests The authors declare no competing interests.

Additional information

Supplementary information The online version contains supplementary material available at https://doi.org/10.1038/s41586-025-10077-z.

Correspondence and requests for materials should be addressed to Jessica A. Lueders-Dumont or Xingchen Tony Wang.

Peer review information *Nature* thanks David Baker, Peter Roopnarine and the other, anonymous, reviewer(s) for their contribution to the peer review of this work.

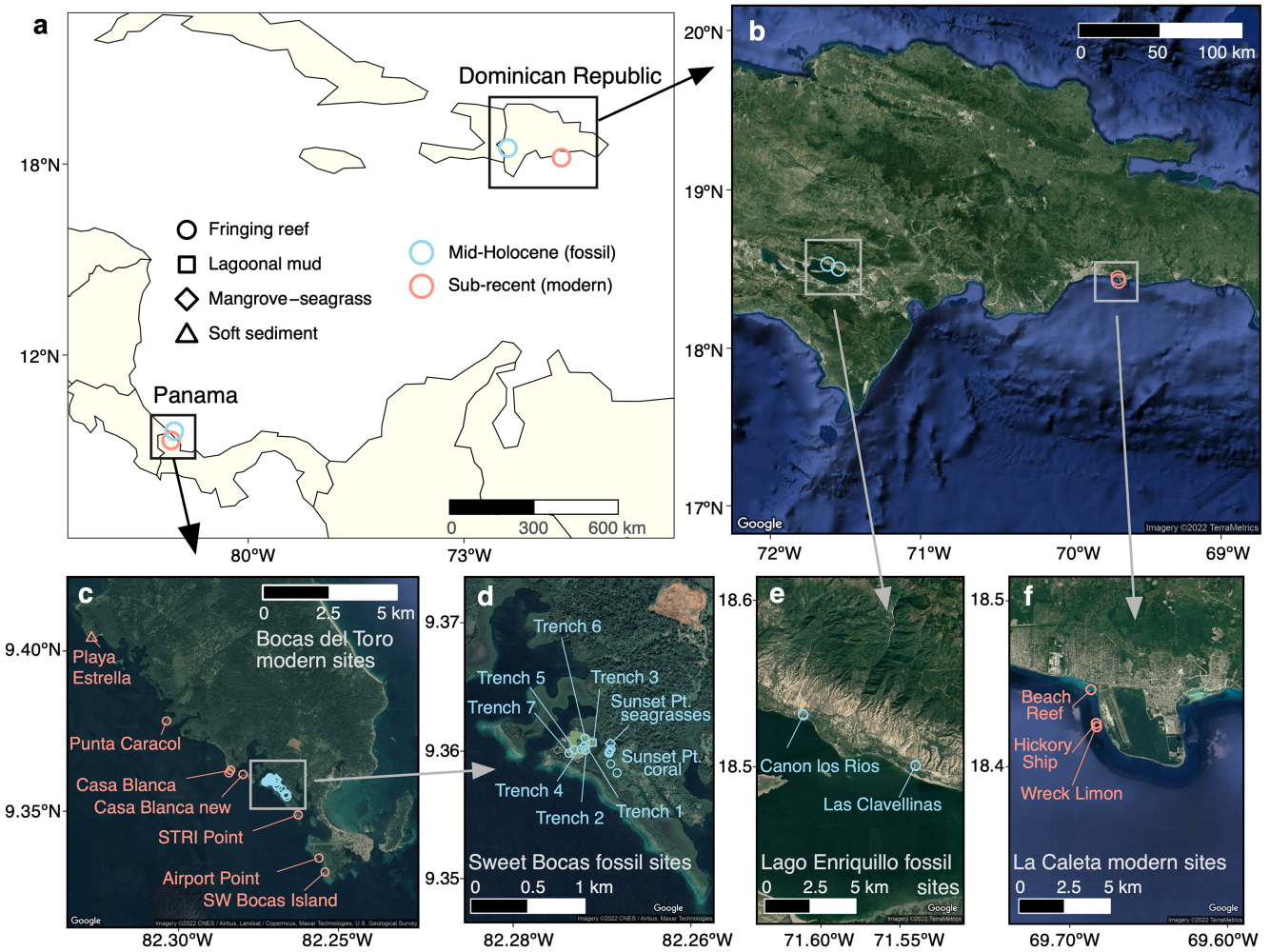

Extended Data Fig. 1 | Detailed maps of localities from which otoliths and corals were measured. a, overview map of the Caribbean Region, **b**, Dominican Republic map showing both fossil and modern localities, **c**, Panama map showing both fossil and modern localities, **d**, zoomed map on Panama fossil localities, **e**, Dominican Republic fossil localities, and **f**, Dominican Republic modern localities. **b**–**f**, Google Earth imagery copyright 2022. All base maps were created using the R package *ggmap*[71] (v.3.0.0).

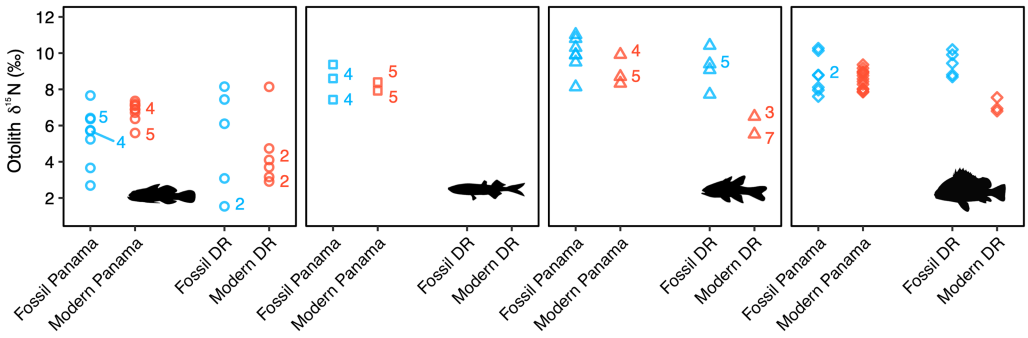

Extended Data Fig. 2 | Number of otoliths analysed for each measurement. All measurements were $n = 1$ otolith other than measurements for which numbers (n) are shown in labelled text, for **a**, gobies, **b**, silversides, **c**, cardinalfishes, and **d**, grunts. Fish silhouettes reproduced from ref. 51, GitHub, under a GPL-2 license.

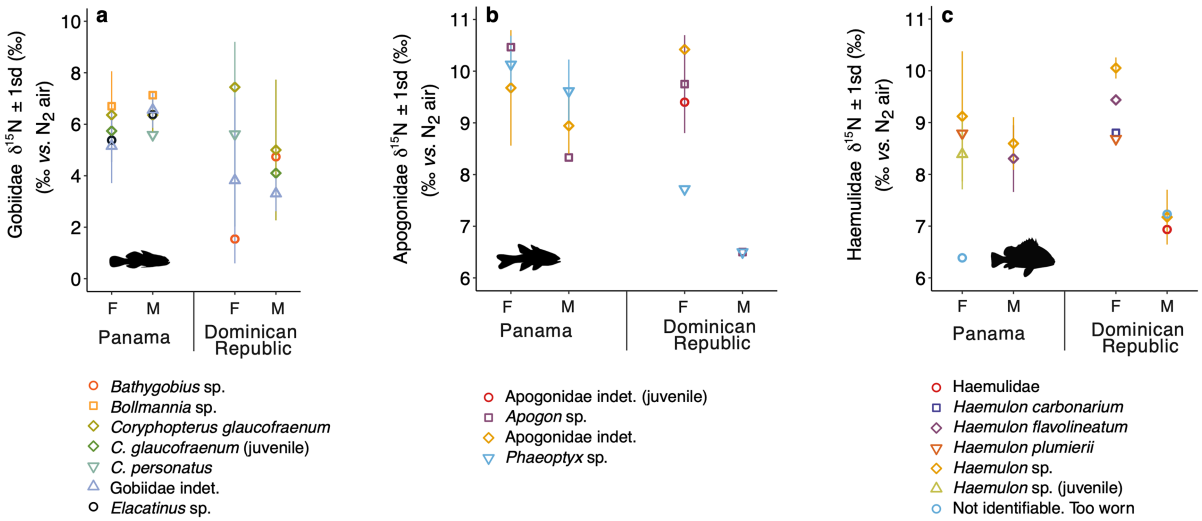

Extended Data Fig. 3 | $\delta^{15}N_{oto}$ (mean ± 1 s.d.) plotted by the most highly taxonomically resolved identification (species, genus, or family). Data shown for **a**, gobies (Gobiidae; $n = 45$ biologically independent samples/ animals), **b**, cardinalfishes (Apogonidae; $n = 40$ biologically independent samples/ animals), and **c**, grunts (Haemulidae; $n = 32$ biologically independent samples/ animals) for fossil (F) and modern (M) time periods. $\delta^{15}N_{oto}$ patterns, which in the main text (Fig. 2) are aggregated by family, are retained at each level of taxonomic identity. Thus, family-specific patterns reported in the main text are representative of more highly resolved taxonomic identity, where available, of fishes in both regions and time periods. Taxonomic identity of all otoliths in the study was challenged by the fact that otoliths of young fishes have not developed some of the diagnostic morphological features, limiting the taxonomic identification of all otoliths to genus or species level. For this reason, the $\delta^{15}N_{oto}$ data in the main text are examined at their coarsest, family-level taxonomic identity. Fish silhouettes reproduced from ref. 51, GitHub, under a GPL-2 license.

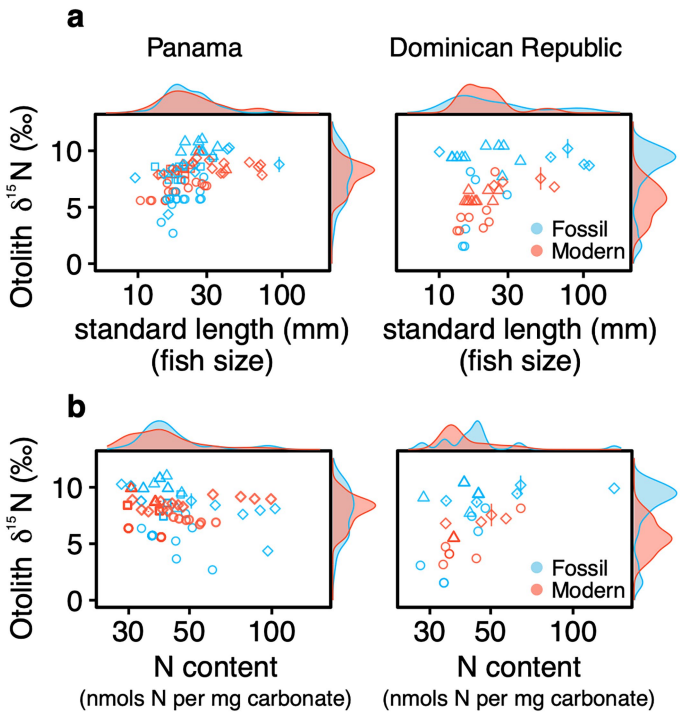

Extended Data Fig. 4 | δ^{15}N versus fish size and versus the N content for each otolith. a, δ^{15}N versus reconstructed fish size. Each symbol corresponds to an individual fish otolith for which fish standard length (mm) was reconstructed. Where error bars are shown, they denote the 1 s.d. of two ($n = 2$) whole-process replicates from the same otolith specimen. A total of $n = 131$ biologically independent otolith specimens were measured for fish length for Panama (44 fossil, 44 modern) and for the Dominican Republic (21 fossil, 22 modern). Fossil and modern fish size (standard length, in mm) did not change in Panama (Wilcoxon, two-sided, $P = 0.796$, $W = 936$, $r = 0.0280$) or the Dominican Republic ($P = 1$, $W = 231$, $r = 0$). For Panama, fossil fish size was 24.2 ± 2.1 mm (1 s.e.) and modern was 26.5 ± 2.1 mm (1 s.e.); the Dominican Republic fossil fish size was 32 ± 4.9 mm (1 s.e.) and modern Dominican Republic was 22.6 ± 4.8 mm (1 s.e.). Symbols shapes as for Fig. 2. See also Supplementary Fig. S4 for intra-family patterns in δ^{15}N versus fish size. **b**, Comparing N content for otoliths shows no difference between time periods for Panama (Wilcoxon, two-sided, $P = 0.13$, $W = 1275$, $r = 0.157$) but does show a difference for the Dominican Republic ($P = 0.03$, $W = 319$, $r = 0.327$) (Extended Data Table 1) (n = 136 biologically independent samples for which fish δ^{15}N and N content were reconstructed for Panama (44 fossil, 49 modern) and the Dominican Republic (21 fossil, 22 modern). For coral N content data, see Extended Data Table 1 and Supplementary Fig. S5.

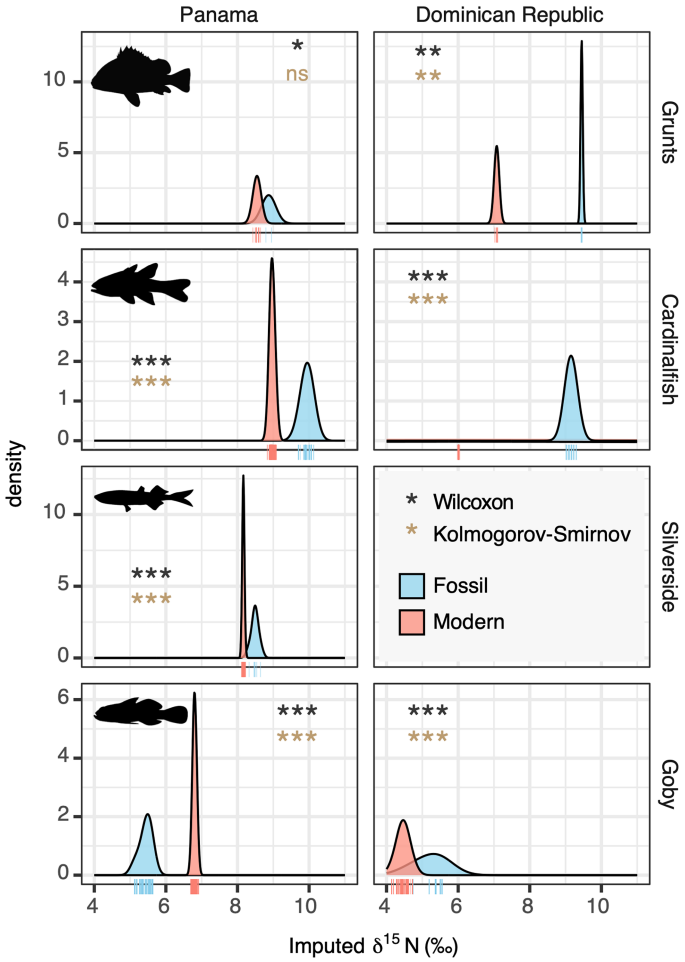

Extended Data Fig. 5 | Distribution and statistical significance of bootstrapped resampling for each family. For Panama, shifts in mean $\delta^{15}N$ were significant for grunts (Wilcoxon, two-sided, $P = 0.033$, $W = 26$, $r = 0.572$), cardinalfishes ($P = 3.3 \times 10^{-26}$, $W = 8281$, $r = 0.722$), silversides ($P = 8.7 \times 10^{-6}$, $W = 1169$, $r = 0.342$), and gobies ($P = 2.1 \times 10^{-216}$, $W = 0$, $r = 0.828$) and shifts in the variance were significant for cardinalfishes (Kolmogorov-Smirnov, two-sided, $P = 2.2 \times 10^{-16}$, $D = 1$), silversides ($P = 2.9 \times 10^{-6}$, $D = 1$), and gobies ($P = 2.2 \times 10^{-16}$, $D = 1$). In the Dominican Republic, shifts in mean $\delta^{15}N$ were significant for grunts ($P = 0.003$, $W = 42$, $r = 0.834$), cardinalfishes ($P = 4.6 \times 10^{-42}$, $W = 4347$, $r = 0.993$), and gobies ($P = 1.9 \times 10^{-47}$, $W = 21732$, $r = 0.840$) and shifts in the variance were significant for grunts ($P = 0.0031$, $D = 1$), cardinalfishes ($P = 2.2 \times 10^{-16}$, $D = 1$), and gobies ($P = 2.2 \times 10^{-16}$, $D = 0.93$) (Extended Data Table 3). Fish silhouettes reproduced from ref. 51, GitHub, under a GPL-2 license.

Extended Data Table 1 | Temporal and regional comparisons of measured $\delta^{15}N_{oto}$ and $\delta^{15}N_{cb}$

a

			$\delta^{15}N$			N content		
comp.	**Variable1** (*n*)	**Variable2** (*n*)	**P adj.**	**signif.**	**statistic**	**P adj.**	**signif.**	**statistic**
time	modern_PAN_coral *(16)*	fossil_PAN_coral *(10)*	0.445	ns	109	0.299	ns	108
time	modern_DR_coral *(4)*	fossil_DR_coral *(5)*	0.619	ns	14	0.375	ns	15
time	modern_PAN_goby *(16)*	fossil_PAN_goby *(15)*	0.153	ns	75	0.605	ns	99
time	modern_DR_goby *(8)*	fossil_DR_goby *(6)*	1	ns	24	0.65	ns	28
time	modern_PAN_silversides *(10)*	fossil_PAN_silversides *(9)*	0.706	ns	50	**$1.9x10^{-4}$**	***	90
time	modern_PAN_cardinal *(10)*	fossil_PAN_cardinal *(10)*	0.163	ns	70	**$1.2x10^{-2}$**	*	85
time	modern_DR_cardinal *(10)*	fossil_DR_cardinal *(10)*	**$2.5x10^{-4}$**	***	100	**$5x10^{-3}$**	**	93
time	modern_PAN_grunts *(13)*	fossil_PAN_grunts *(10)*	0.828	ns	61	0.871	ns	69
time	modern_DR_grunts *(4)*	fossil_DR_grunts *(6)*	**0.048**	*	20	0.871	ns	14
region	fossil_PAN_coral *(10)*	fossil_DR_coral *(5)*	0.962	ns	23	0.679	ns	29
region	fossil_PAN_goby *(15)*	fossil_DR_goby *(6)*	1	ns	42	0.605	ns	36
region	fossil_PAN_cardinal *(10)*	fossil_DR_cardinal *(10)*	0.129	ns	27	0.218	ns	68
region	fossil_PAN_grunts *(10)*	fossil_DR_grunts *(6)*	0.151	ns	38	0.871	ns	30
region	modern_PAN_coral *(16)*	modern_DR_coral *(4)*	0.962	ns	31	0.298	ns	14
region	modern_PAN_goby *(16)*	modern_DR_goby *(8)*	**0.02**	*	16	0.555	ns	42
region	modern_PAN_cardinal *(10)*	modern_DR_cardinal *(10)*	**$2.5x10^{-4}$**	***	0	0.256	ns	35
region	modern_PAN_grunts *(13)*	modern_DR_grunts *(4)*	**$5x10^{-3}$**	**	0	0.871	ns	28

b

			$\delta^{15}N$			N content		
comp.	**Variable1** (*n*)	**Variable2** (*n*)	**P adj.**	**signif.**	**statistic**	**P adj.**	**signif.**	**statistic**
time	modern_PAN_all_oto *(49)*	fossil_PAN_all_oto *(45)*	0.972	ns	1083	0.13	ns	1275
time	modern_DR_all_oto *(22)*	fossil_DR_all_oto *(21)*	**$1.5x10^{-4}$**	***	387	**0.03**	*	319

a, Results of pairwise Wilcoxon statistical tests for measured $\delta^{15}N_{oto}$ (otolith-bound proteins), $\delta^{15}N_{cb}$ (coral skeletal-bound proteins), and N content for each intra-taxon comparison are shown (Benjamini-Hochberg *P* adjust method for all comparisons); **b**, Results of Wilcoxon statistical tests (not pairwise, and thus not corrected for multiple comparisons) for measured $\delta^{15}N_{oto}$ and N content are shown for Panama and the Dominican Republic (DR).

Extended Data Table 2 | Summary statistics for mean $\delta^{15}N$, food chain length (FCL), and mean trophic level (MTL)

	Fossil $\delta^{15}N$ ± 1 s.d. (‰)	Modern $\delta^{15}N$ ± 1 s.d. (‰)	$\delta^{15}N$ change (‰)	FCL decline *vs.* fossil (%)	adjusted Wilcoxon *P*, statistic (*W*), effect size (*r*)	Modern $\delta^{15}N$ (baseline corrected)	$\delta^{15}N$ change (‰) *vs.* fossil (baseline corrected)
Panama							
Coral	5.07 ± 0.91	4.58 ± 0.41	-0.49		P=0.445, W=109, r=0.3	5.07	0
Goby	5.57 ± 1.13	6.42 ± 0.66	0.85		P=0.153, W=75, r=0.321	6.91	1.34
Silverside	8.17 ± 0.74	8.16 ± 0.25	-0.01		P=0.706, W=50, r=0.096	8.65	0.48
Cardinalfish	10.02 ± 0.83	9.15 ± 0.67	-0.86		P=0.163,W=70, r=0.342	9.64	-0.38
Grunt	8.35 ± 1.65	8.55 ± 0.51	0.20		P=0.828,W=61, r=0.052	9.04	0.68
Taxon-mean FCL[a] (measured)	*4.45 ± 1.41*[b]	*2.73 ± 0.94*[b]	*-1.72*	*39%*		*2.73*	
Taxon-mean MTL[a] (measured)	*8.02 ± 0.66*[b]	*8.07 ± 0.30*[b]	*0.05*		P=1.0, W=8, r=0	*8.56*	*0.54*
Family abundance-weighted MTL[c] (bootstrapped)	*5.84 ± 1.3*	*7.15 ± 0.79*	***1.32***		***P=2.2x10^{-16},** W=567, r=0.669	*7.64*	*1.80*
Dominican Republic							
Coral	4.99 ± 0.60	4.60 ± 0.39	-0.39		P=0.619,W=14, r=0.33	4.99	0
Goby	4.64 ± 2.96	4.22 ± 1.71	-0.42		P=1,W=24, r=0	4.61	-0.03
Cardinalfish	9.51 ± 0.81	5.81 ± 0.47	**-3.69**		***P=2.5x10^{-4},** W=100, r=0.873	6.21	-3.30
Grunt	9.54 ± 0.86	7.12 ± 0.32	**-2.42**		***P=0.048,** W=20, r=0.82	7.51	-2.02
Taxon-mean FCL[a] (measured)	*4.90 ± 3.10*[b]	*2.90 ± 1.74*[b]	*-1.99*	*40%*		*2.90*	
Taxon-mean MTL[a] (measured)	*7.90 ± 1.07*[b]	*5.72 ± 0.53*[b]	*-2.18*		P=0.4, W=7, r=0.445	*6.11*	*-1.79*
Family abundance-weighted MTL[c] (bootstrapped)	*6.05 ± 1.97*	*5.24 ± 0.82*	***-0.81***		***P=8.4x10^{-5},** W=33018, r=0.176	*5.63*	*-0.42*

FCL was calculated as the range of taxon-specific means. Measured MTL was calculated as the mean of $\delta^{15}N_{oto}$ for each family. Baseline-corrected $\delta^{15}N$ were standardized by the regional (Panama or Dominican Republic) and temporal $\delta^{15}N_{cb}$ patterns. Wilcoxon (two-sided, Benjamini-Hochberg adjusted) *P*-values and effect sizes (*r*) are shown. Bolded cells indicate significant temporal differences.

Extended Data Table 3 | Statistical tests for family-level bootstrapped $\delta^{15}N$ metrics

a

Bootstrapped family mean $\delta^{15}N$ (trophic level): model results

Region	Family	Fossil (‰)	Modern (‰)	$\delta^{15}N$ change (‰)	Fossil *n*	Modern *n*	Wilcoxon *P*, statistic (*W*), effect size (*r*)
Panama	Goby	5.44	6.80	**1.4**	508	935	***$P=2.1x10^{-216}$, W=0, r=0.828
	Silverside	8.49	8.16	**-0.3**	7	167	***$P=8.7x10^{-6}$, W=1169, r=0.342
	Cardinalfish	9.94	8.97	**-1.0**	49	169	***$P=3.3x10^{-26}$, W=8281, r=0.722
	Grunt	8.87	8.54	**-0.3**	2	13	***P=0.033**,W=26, r=0.572
Dominican Republic	Goby	5.22	4.46	**-0.8**	126	174	***$P=1.9x10^{-47}$, W=21732, r=0.840
	Cardinalfish	9.15	6.01	**-3.1**	27	161	***$P=4.6x10^{-42}$, W=4347, r=0.993
	Grunt	9.45	7.08	**-2.4**	6	7	**P=0.003**, W=42, r=0.834

b

Bootstrapped family variations in $\delta^{15}N$ (niche width): model results

Region	Family	Fossil (‰)	Modern (‰)	ratio of s.d.	% decline	Fossil *n*	Modern *n*	F test P-val, df, variance ratio (95% CI)	Kolmogorov-Smirnov (*P*, *D*)
Panama	Goby	0.151	0.046	3.28	70%	508	935	***$P=2.2x10^{-16}$, df=507, df=934, ratio var=10.8 (9.3-12.6)	***$P=2.2x10^{-16}$, D=1
	Silverside	0.095	0.020	4.75	79%	7	167	***$P=2.2x10^{-16}$, df=6, df=166, ratio var=22.1 (8.9-108.0)	***$P=2.9x10^{-6}$, D=1
	Cardinalfish	0.109	0.053	2.06	51%	49	169	***$P=4.0x10^{-12}$, df=48, df=168, ratio var=4.2 (2.8-6.9)	***$P=2.2x10^{-16}$, D=1
	Grunt	0.110	0.056	1.96	49%	2	13	$P=0.14^{ns}$, df=1, df=12, ratio var=3.9 (0.6-3820.2)	$P=0.062^{ns}$, D=1
Dominican Republic	Goby	0.321	0.145	2.21	55%	126	174	***$P=2.2x10^{-16}$, df=125, df=173, ratio var=4.9 (3.6-6.8)	***$P=2.2x10^{-16}$, D=0.93
	Cardinalfish	0.088	0.000	NA	100%	27	161	***$P=2.2x10^{-16}$, df=26, df=160, ratio var=inf	***$P=2.2x10^{-16}$, D=1
	Grunt	0.012	0.029	0.41	-142%	6	7	$P=0.07^{ns}$, df=5, df=6, ratio var=0.17 (0.028-1.2)	**P=0.0031, D=1

a, Bootstrapped results of mean $\delta^{15}N$ (Wilcoxon, using Benjamini-Hochberg *P* adjust method for all comparisons). **b**, Bootstrapped results of $\delta^{15}N$ variation. See Extended Data Fig. 5 for $\delta^{15}N$ distributions and Supplementary Table S5 for the isotopic and taxonomic data used to impute the bootstrapped $\delta^{15}N$.

Extended Data Table 4 | Summary statistics for niche width and variance comparisons of measured $\delta^{15}N$ across time periods within each family

	Fossil niche width (1 s.d., ‰)	Modern niche width (1 s.d., ‰)	Ratio of variance (95% CI)	Percent decline compared to fossil (%)	F test to compare variances (*P*, *df*)	Brown-Forsythe (*P*, *F*)	Fligner-Killeen, homogeneity of variances (*P*, χ^2)
Panama							
Coral	0.86	0.44	4.9 (1.1-20.5)	49%	***P=0.05**, df=9, df=15	P=0.18, Fstat=2.44	****P=0.007,** χ^2=10.3
Goby	1.13	0.66	3.0 (1.0-8.8)	42%	***P=0.05**, df=14, df=15	***P=0.05**, Fstat=6.43	P=0.71, χ^2=0.33
Silverside	0.74	0.25	8.5 (2.1-37,2)	66%	****P=0.01**, df=8, df=9	P=0.98, Fstat=4.6×10^{-4}	P=0.45, χ^2=1.2
Cardinalfish	0.83	0.67	1.5 (0.4-6.2)	19%	P=0.54, df=9, df=9	***P=0.05,** Fstat=6.57	P=0.81, χ^2=0.058
Grunt	1.65	0.51	10.4 (3.0-40.1)	69%	****P=0.002**, df=9, df=12	P=0.18, Fstat=0.132	P=0.45, χ^2=2.18
Dominican Republic							
Coral	0.60	0.39	2.3	34%	P=0.52, df=4, df=3	P=0.37, Fstat=1.40	P=0.58, χ^2=0.31
Goby	2.96	1.71	3.0	42%	P=0.24, df=5, df=7	P=0.76, Fstat=0.097	P=0.22, χ^2=3.66
Cardinalfish	0.81	0.47	2.9	42%	P=0.24, df=9, df=9	*****P=4.05×10^{-8}**, Fstat=154	P=0.23, χ^2=2.07
Grunt	0.87	0.32	7.2	63%	P=0.24, df=4, df=3	****P=0.004**, Fstat=33.3	P=0.23, χ^2=1.82

Ratio of variances was assessed using the F test (two-sided; *P, F, df*), with comparisons of homogeneity of variance from the one-sided Brown-Forsythe (parametric, robust to non-normality; *P, F*) and the two-sided Fligner-Killeen (non-parametric; *P*, χ^2) tests, which together assess whether group variances differ. *P*-values were adjusted for multiple comparisons using the Benjamini-Hochberg method.

Extended Data Table 5 | Statistical tests for community metrics as calculated with bootstrapped $\delta^{15}N$

	n	Min (‰)	Max (‰)	MTL (‰)	1 s.d. (‰)	Wilcox *P*, statistic (*W*), effect size (*r*)	t.test *P*, statistic (*t*)	FCL from 95% IQR (‰)	FCL decline *vs.* fossil (‰)	F-test (Var test)	Kolmogorov-Smirnov test (*P*, *D*)	Kurtosis	Skewness
Panama													
Fossil	559	5.13	10.10	5.84	1.3			4.89				2.79	8.95
Modern	1117	6.70	9.09	7.15	0.79			2.32	52.6%			1.83	4.38
						*** **P=2.2e^{-16}**, W=56693, r=0.669	*** **P=2.2e^{-16}**, t=-21.9, df=772.61			*** **P=2.2e^{-16}**, F=2.68, df=558, ratio var=2.67	*** **P=2.2e^{-16}**, D=0.91		
Dominican Republic													
Fossil	159	4.73	9.46	6.05	1.97			4.72				1.33	2.98
Modern	342	4.14	7.11	5.24	0.82			1.87	60.4%			0.13	1.40
						*** **P=8.4e^{-5}**, W=33018, r=0.176	*** **P=2.2e^{-8}**, t=5.84, df=195.18			*** **P=2.2e^{-16}**, F=4.04, df=158, ratio var=4.05	*** **P=2.2e^{-16}**, D=0.47		

To estimate the Food Chain Length (FCL) from the bootstrapped and smoothed distributions in Fig. 3d, the interquartile range (IQR=95%) was used. The modern FCL decline (‰) was calculated, as well as the kurtosis and skewness of each distribution. Statistical tests for differences in variation (two-sided F-test for variation) and distribution (two-sided Kolmogorov-Smirnov) were conducted using R.

nature portfolio

Corresponding author(s): Jessica Lueders-Dumont

Last updated by author(s): Feb 5, 2026

Reporting Summary

Nature Portfolio wishes to improve the reproducibility of the work that we publish. This form provides structure for consistency and transparency in reporting. For further information on Nature Portfolio policies, see our Editorial Policies and the Editorial Policy Checklist.

Statistics

For all statistical analyses, confirm that the following items are present in the figure legend, table legend, main text, or Methods section.

n/a	Confirmed	
☐	☒	The exact sample size (*n*) for each experimental group/condition, given as a discrete number and unit of measurement
☐	☒	A statement on whether measurements were taken from distinct samples or whether the same sample was measured repeatedly
☐	☒	The statistical test(s) used AND whether they are one- or two-sided *Only common tests should be described solely by name; describe more complex techniques in the Methods section.*
☐	☒	A description of all covariates tested
☐	☒	A description of any assumptions or corrections, such as tests of normality and adjustment for multiple comparisons
☐	☒	A full description of the statistical parameters including central tendency (e.g. means) or other basic estimates (e.g. regression coefficient) AND variation (e.g. standard deviation) or associated estimates of uncertainty (e.g. confidence intervals)
☒	☐	For null hypothesis testing, the test statistic (e.g. *F*, *t*, *r*) with confidence intervals, effect sizes, degrees of freedom and *P* value noted *Give P values as exact values whenever suitable.*
☒	☐	For Bayesian analysis, information on the choice of priors and Markov chain Monte Carlo settings
☒	☐	For hierarchical and complex designs, identification of the appropriate level for tests and full reporting of outcomes
☐	☒	Estimates of effect sizes (e.g. Cohen's *d*, Pearson's *r*), indicating how they were calculated

Our web collection on statistics for biologists contains articles on many of the points above.

Software and code

Policy information about availability of computer code

Data collection	Thermo Fisher Scientific Isotope Ratio Mass Spectrometry Software (Isodat version 3.0). ImageJ (version: 1.52k).
Data analysis	All data analysis was conducted in the software R (version: 4.1.2) using the following packages: tidyverse (version: 1.3.1), boot (version: 1.3-28), rlist (version: 0.4.6.2), onewaytests (version: 2.7), rstatix (version: 0.7.0), forcats (version: 0.5.1), and tidyr (version: 1.3.1) packages. For other statistical and mapping operations in R, we used ggmap (version: 3.0.0), ggrepel (version: 0.9.3), ggsn (version: 0.5.3), cowplot (version: 1.1), grid (version: 4.1.1), and fishualize (version: 0.2.3).

For manuscripts utilizing custom algorithms or software that are central to the research but not yet described in published literature, software must be made available to editors and reviewers. We strongly encourage code deposition in a community repository (e.g. GitHub). See the Nature Portfolio guidelines for submitting code & software for further information.

Data

Policy information about availability of data

All manuscripts must include a data availability statement. This statement should provide the following information, where applicable:

- Accession codes, unique identifiers, or web links for publicly available datasets
- A description of any restrictions on data availability
- For clinical datasets or third party data, please ensure that the statement adheres to our policy

All the raw data supporting the findings of this study are publicly available on figshare (https://10.6084/m9.figshare.28811663).

Research involving human participants, their data, or biological material

Policy information about studies with human participants or human data. See also policy information about sex, gender (identity/presentation), and sexual orientation and race, ethnicity and racism.

Reporting on sex and gender	N/A
Reporting on race, ethnicity, or other socially relevant groupings	N/A
Population characteristics	N/A
Recruitment	N/A
Ethics oversight	N/A

Note that full information on the approval of the study protocol must also be provided in the manuscript.

Field-specific reporting

Please select the one below that is the best fit for your research. If you are not sure, read the appropriate sections before making your selection.

☐ Life sciences ☐ Behavioural & social sciences ☒ Ecological, evolutionary & environmental sciences

For a reference copy of the document with all sections, see nature.com/documents/nr-reporting-summary-flat.pdf

Ecological, evolutionary & environmental sciences study design

All studies must disclose on these points even when the disclosure is negative.

Study description	In this study, we measured nitrogen isotope abundances from preserved proteins of taxonomically-diagnostic fish ear stones (otoliths) and from preserved proteins of coral skeletons. Otolith and coral specimens were collected from pre-historical and modern coral sedimentary deposits from two distinct regions of the Caribbean Sea. With the resulting data, we were able to compare fish dietary patterns from pre-human-disturbance coral reefs and modern reefs, demonstrating the human influence on fish foraging behavior and energy flow on modern, human-impacted Caribbean coral reefs.
Research sample	136 fish otoliths (45 gobies, 40 cardinalfish, 19 silversides, 32 grunts) and 35 coral fragments were measured. Fish families were chosen for their distinct ecological roles from one another on coral reefs and for their high otolith abundances compared to other taxa in the sedimentary record. Coral species Porites furcata was chosen because members of this coral family (Poritidae) are robust archives of changes in the nitrogen isotope composition of primary producers in coral reef environments. Otolith samples are meant to provide the population-level patterns in fish foraging behavior for each family. Coral samples represent a spatially- and temporally-comparable archive to otoliths, providing a control for non-dietary nitrogen isotope differences between regions or time periods.
Sampling strategy	No statistical methods were used to predetermine samples sizes. To select otoliths for isotope analysis, specimens were randomly chosen from sub-localities within each region until n = 10-30 otoliths of each taxon from each region and time period were selected where available. Our sampling strategy focused on obtaining samples from a wide distribution of sub-localities within each region, with the rationale of capturing as much potential variability within each region and time period as possible. For protein extraction and isotopic analysis of otoliths weighing 0.06 mg to 5.5 mg, the whole sample was used. Otoliths >5.5 mg were crushed, homogenized, and subsampled to 4.0 ± 0.5 mg. Initial N isotope analyses involved pooled otoliths out of an abundance of caution to ensure sufficient N (i.e., >5nmol of nitrogen) for analysis. Subsequently, all isotopic analyses were conducted on individual otoliths as even the smallest specimens (otoliths as small as 0.06 mg) yielded sufficient nitrogen for isotope analysis .
Data collection	Isotope Ratio Mass Spectrometry, ImageJ.
Timing and spatial scale	Data collection was not time dependent. The sediment samples were collected between 2012 and 2014.
Data exclusions	No measurements were excluded.
Reproducibility	All batches of isotopic measurements included analyses of internationally-recognized standards and sample replicate analyses.
Randomization	Samples were organized by region and time period.
Blinding	Blinding was not relevant to the study design. The only extent of blinding was that the locality and time period associated with each specimen was not known during isotope analysis--only the taxonomic identity (based on otolith shape and sampleID).

Did the study involve field work? ☒ Yes ☐ No

Field work, collection and transport

Field conditions	Otoliths and coral specimens were obtained from SCUBA-based sampling of modern coral reefs and from sedimentary sampling of fossil mid-Holocene coral reef deposits. For both the modern and fossil reef sampling, bulk sediments, ~9 kg per sample, were collected from reef frameworks using different methods depending on the time period. In the mid-Holocene sites, sediments were excavated from 3 m deep trenches, while in modern reefs, SCUBA divers collected sediment from 10–15 cm deep strata adjacent to living corals under water depths of 2–19 m. Sediment samples were sieved into size fractions (2 mm, 500 µm, 250 µm, and 106 µm) and then otoliths were manually extracted under a dissecting microscope. Otoliths were identified to their highest taxonomic resolution through comparisons with a region-specific modern otolith reference collection.
Location	Field sites were in the southeast Dominican Republic (-69.7, 18.5) and in Caribbean Panama (-82.3, 9.4).
Access & import/export	Collection permits for bulk sediment sampling of modern and mid-Holocene reefs were issued by the Ministerio de Ambiente, República de Panamá (Permit number SE/AO-4-18) and the Ministerio de Medio Ambiente y Recursos Naturales, República Dominicana (Permit number VAPB-02374).
Disturbance	In the case of the fossil reef site in Panama, disturbance was minimized by sampling sediments within a site where excavation was already being carried out for development of a hotel and resort. For the fossil site in the Dominican Republic, disturbance was minimized by sampling within exposed storm channels in the Enriquillo Basin. For modern reef sedimentary sampling in both regions, sediments were sampled adjacent to living coral but did not disturb the living coral.

Reporting for specific materials, systems and methods

We require information from authors about some types of materials, experimental systems and methods used in many studies. Here, indicate whether each material, system or method listed is relevant to your study. If you are not sure if a list item applies to your research, read the appropriate section before selecting a response.

Materials & experimental systems

n/a	Involved in the study
☒	☐ Antibodies
☒	☐ Eukaryotic cell lines
☐	☒ Palaeontology and archaeology
☒	☐ Animals and other organisms
☒	☐ Clinical data
☒	☐ Dual use research of concern
☒	☐ Plants

Methods

n/a	Involved in the study
☒	☐ ChIP-seq
☒	☐ Flow cytometry
☒	☐ MRI-based neuroimaging

Palaeontology and Archaeology

Specimen provenance	Collection permits for bulk sediment sampling of modern and mid-Holocene reefs were issued by the Ministerio de Ambiente, República de Panamá (Permit number SE/AO-4-18) and the Ministerio de Medio Ambiente y Recursos Naturales, República Dominicana (Permit number VAPB-02374).
Specimen deposition	All otoliths measured destructively for stable isotope analysis were photographed prior to analysis, and the resulting images will be available on FigShare (https://10.0.23.196/m9.figshare.28811663). All additional otoliths from the same collections are available at the Naos Marine Laboratories of the Smithsonian Tropical Research Institute (STRI), Panama, under the category "otolith" without specimen numbers.
Dating methods	No new dates were obtained for this study.

☒ Tick this box to confirm that the raw and calibrated dates are available in the paper or in Supplementary Information.

Ethics oversight	Permits for bulk sediment sampling were issued by the Ministerio de Ambiente, República de Panamá and the Ministerio de Medio Ambiente y Recursos Naturales, República Dominicana. Ethical approval was not required for this study.

Note that full information on the approval of the study protocol must also be provided in the manuscript.

Plants

Seed stocks	N/A
Novel plant genotypes	N/A
Authentication	N/A